Understanding Data from Incomplete Inter-Point Distance via Locally Low-rank matrix completion and Geometric PDEs

Rongjie Lai
Rensselaer Polytechnic Institute

Joint with Jia Li, Abiy Tasissa@ RPI

Motivation and problems

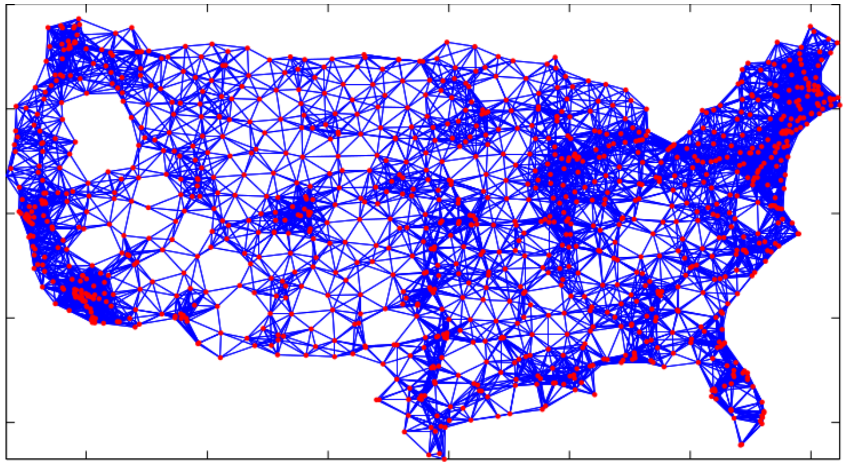

- Global configuration from incomplete information

A network of sensors collaboratively measuring some quantity, the distance matrix is noisy and incomplete

A. Single'08

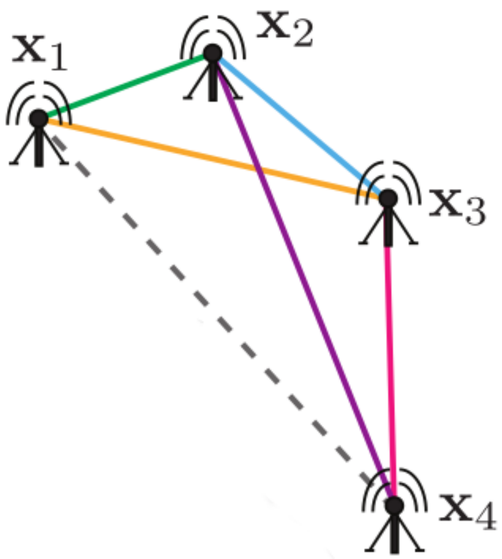

- Protein Structuring

The nuclear magnetic resonance (NMR) spectroscopy provides distance between pairs of hydrogen atoms in a protein.

The measure is incomplete and noisy.

Can we understand the protein structure based on the incomplete measurement without reconstruction?

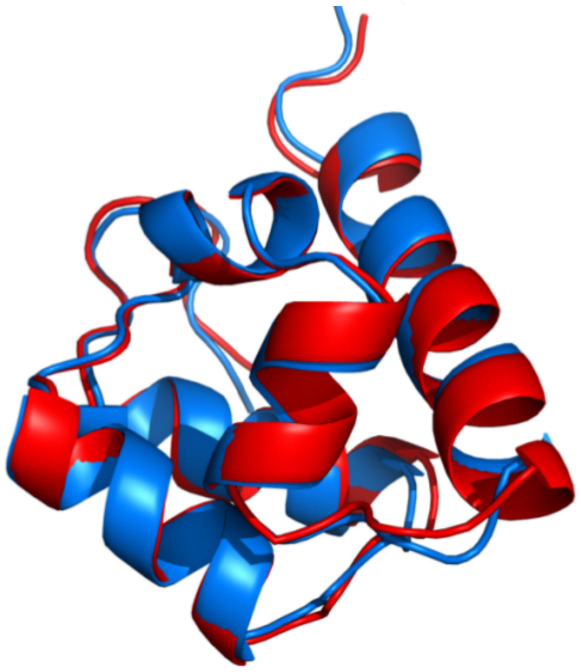

Motivation and problems

Assumption: Given an incomplete distance matrix $D = (d_{ij}^2)$, where $d_{ij} = dist(x_i, x_j)$ for a given point set $\{x_1, \cdots, x_n\}$ sampled on a manifold $\mathcal{M} \subset R^D$.

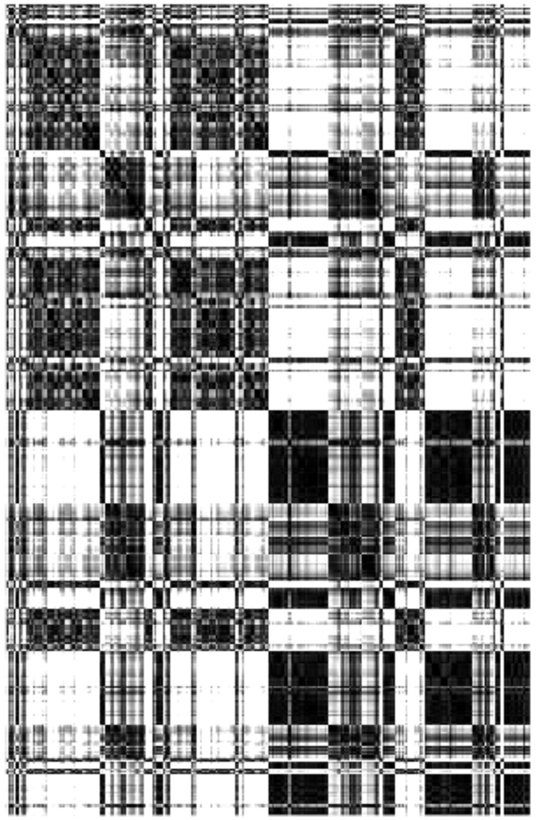

Complete distance

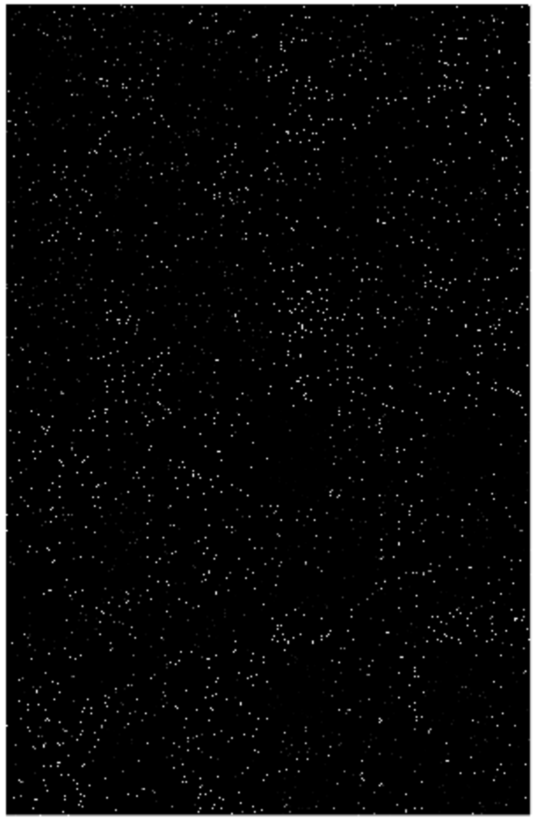

1%

Motivation and problems

Besides visualization, what geometric information can we have for data **without** having global coordinate reconstruction?

Global Recognition

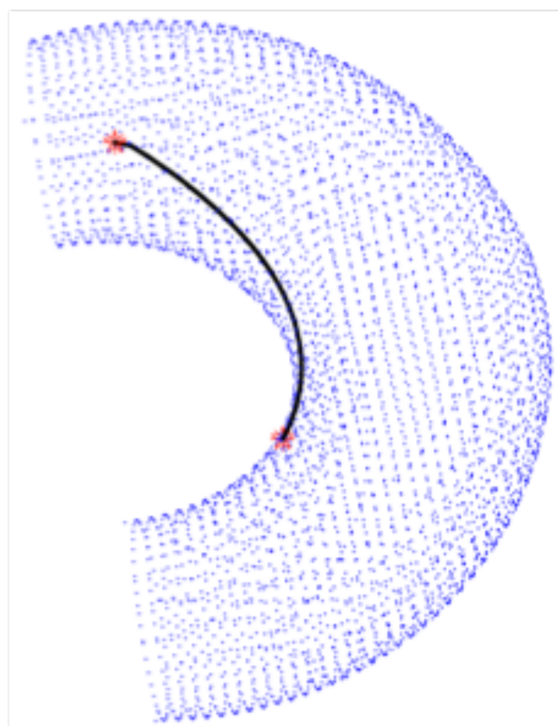

Intrinsic distance

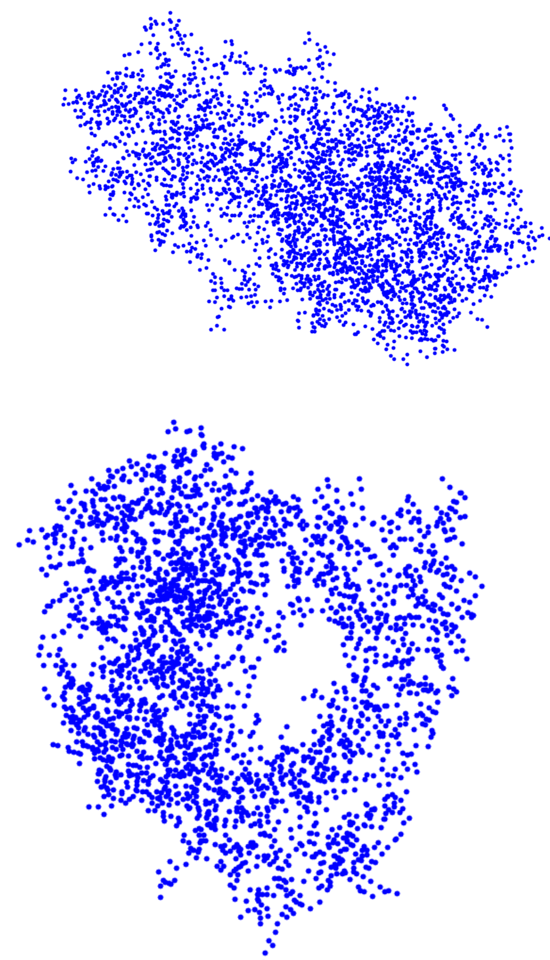

Classification

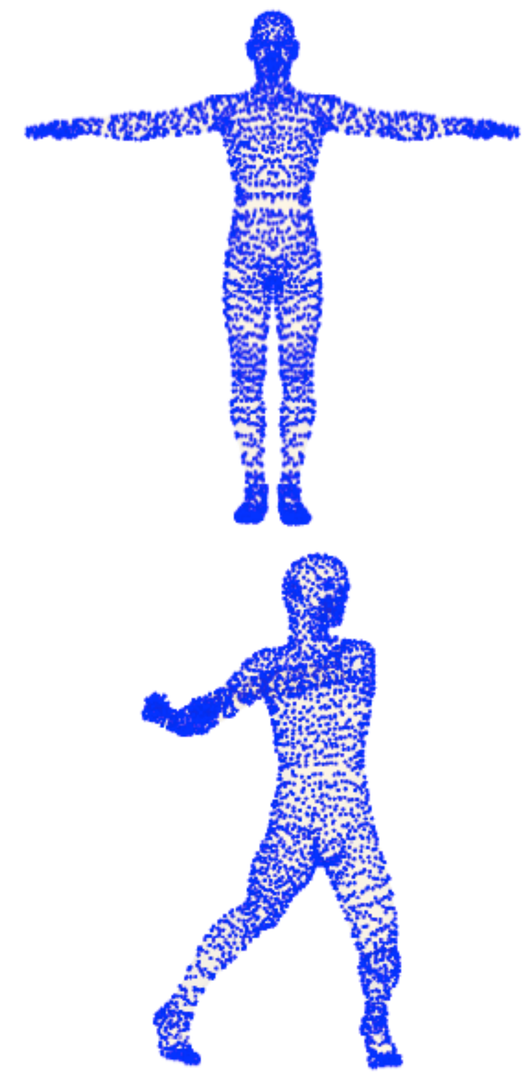

Intrinsic comparison

Challenges

Unlike signals or images

- No global coordinates, only inter-point distance information is given and is with possible missing values and noise.

- No natural or good global parametrization that reveals intrinsic dimensionality and global structure.

- Highly unstructured geometric object in high dimension, difficult to analysis, organize, …. No natural basis for representation.

Our strategy

- Coherent structure inspires us to model distance data for points sampled from manifolds, where local structure can be extracted.

- Geometric PDEs on manifolds can be useful to ”connect the dots” and reveal global structure and provide geometric understanding of data and the underlying manifolds.

No global coordinates reconstruction

Local Recon using low-rank matrix completion → **Solve geometric PDEs based on local recon** → **Conduct understanding based on solutions of PDEs**

Euclidean distance geometry (EDG) problem and matrix completion

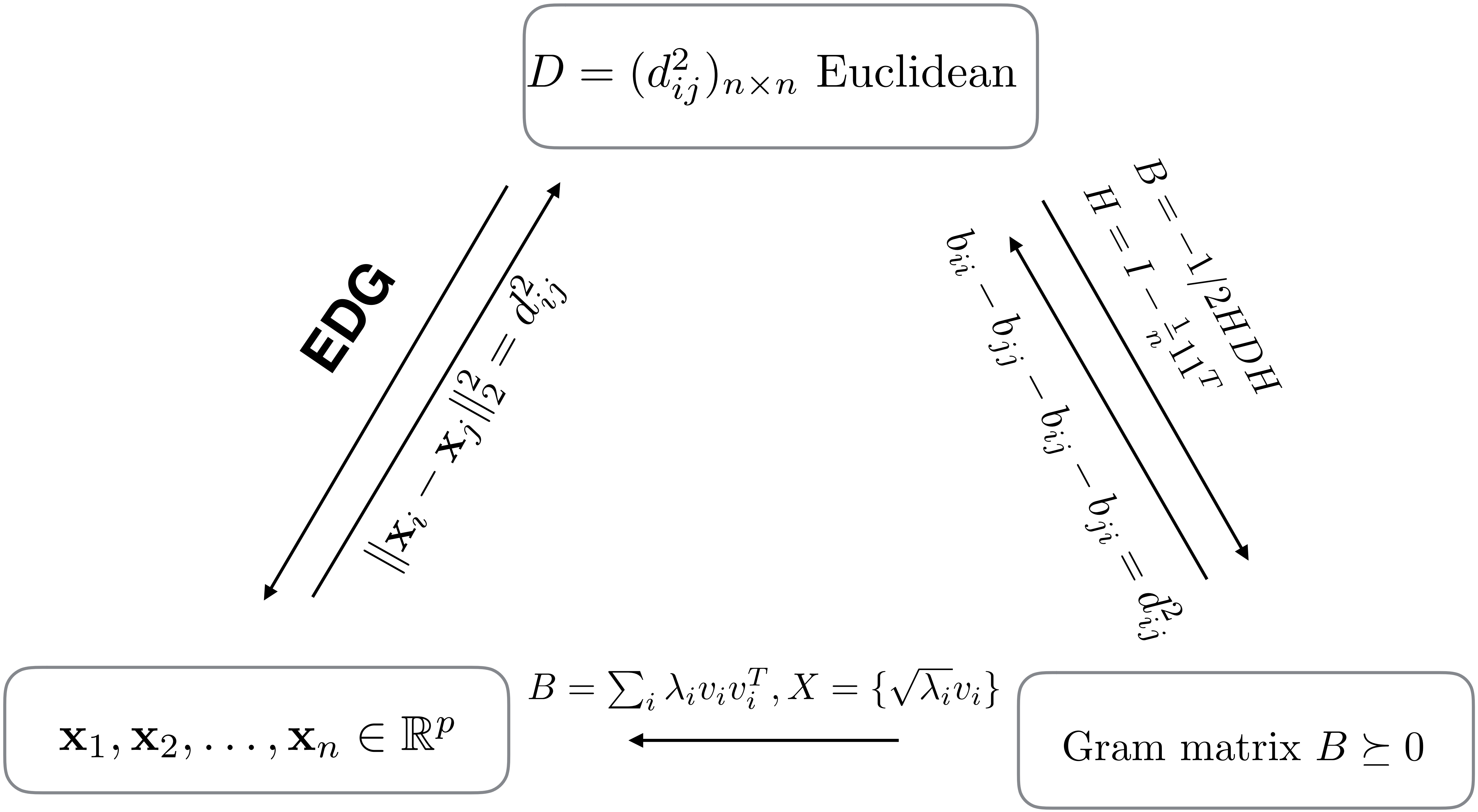

Euclidean distance geometry (EDG) problem and matrix completion

Let write $\Omega \subset \{(i,j) \mid i,j = 1,\cdots,n\}$ as the index set for available values of D. We consider the following matrix completion model to recover the Gram matrix B based on matrix completion theory [Candes-Recht'09,Recht-Fazel-Parrilo'10]

$$\min_{B \succeq 0} \|B\|_* \quad \text{s.t.} \quad \begin{cases} b_{ii} + b_{jj} - 2b_{ij} = d_{ij}^2, & (i,j) \in \Omega \\ \sum_j B_{i,j} = 0, & \forall 1 \leq i \leq n \end{cases}$$

- Instead of reconstructing D, we consider to reconstruct B as it has lower rank.
- The constraint $\sum_j B_{i,j} = 0$ is to remove possible ambiguity due to translation.

Local coordinate reconstruction via Non-orthogonal basis sensing

- Let $\mathcal{S} = \{X = X^T, X1 = 0\}$, we rewrite the EDG relation $B_{i,i} + B_{jj} - B_{ij} - B_{ji} = D_{ij}, \sum_j B_{ij} = 0$ under an appropriate basis $\{\mathbf{w}_{ij} = \mathbf{e}_{ii} + \mathbf{e}_{jj} - \mathbf{e}_{ij} - \mathbf{e}_{ji} \mid i > j\}$.
- The dual basis of $\mathbf{w}_{ij}$ can be written as $\mathbf{v}_{ij} = \sum_{kl} H^{ij,kl}\mathbf{w}_{kl}$ with $H_{ij,kl} = \langle \mathbf{w}_{ij}, \mathbf{w}_{kl}\rangle$. Any $X \in \mathcal{S}$ can be written as $X = \sum_{ij}\langle X, , \mathbf{w}_{ij}\rangle \mathbf{v}_{ij}$.
- Define $\mathcal{R}_\Omega(X) = \dfrac{L}{m} \displaystyle\sum_{(ij)\in\Omega} \langle X\, , \mathbf{w}_{ij}\rangle \mathbf{v}_{ij}$, then the EDG nuclear minimization problem as

$$\underset{B\in\mathcal{S}\cap\{X\succeq 0\}}{\text{minimize}} \quad \|B\|_* \quad \text{s.t. } \mathcal{R}_\Omega(B) = \mathcal{R}_\Omega(B_T)$$

Local coordinate reconstruction via Non-orthogonal basis sensing

1. Entry sensing is under a special orthnormal basis $\{\mathbf{e}_{ij}\}$ [Candes-Recht'09].

2. Sensing under general orthonormal basis is consider in [Gross'11]

3. Restricted isometry property (RIP) is considered for general linear constraint [Recht-Fazel-Parrilo'10], but hard to check the RIP condition.

Definition 1. *The $n \times n$ matrix B_T has coherence ν with respect to basis $\{\mathbf{w}_\alpha\}_{n=1}^{L}$ and $\{\mathbf{v}_\alpha\}_{n=1}^{L}$ if the following estimates hold*

$$\max_{ij} \quad ||\mathcal{P}_{\mathcal{T}}\,\mathbf{w}_{ij}||_F^2 \leq 8\nu\frac{r}{n}, \quad \textit{and} \quad \max_{ij} \quad ||\mathcal{P}_{\mathcal{T}}\,\mathbf{v}_{ij}||_F^2 \leq 32\nu\frac{r}{n}$$

where $\mathcal{P}_{\mathcal{T}}$ is the projection to the tangent space $\mathcal{T} = \{UP + QU^T\}$ of the rank r manifold at $B_T = UDU^T$.

Theorem 1. *If $|\Omega| \geq O\left(rn\nu(1+\beta)\log^2 n\right)$, for $\beta > 1$, the solution to the above problem is unique and equal to B_T with probability atleast $1 - n^{-\beta}$.*

Numerical method for coordinate reconstruction

Define $\mathcal{A} : \mathbb{R}^{n\times n} \to \mathbb{R}^{|\Omega|} \times \mathbb{R}^n : B \mapsto \Big(\{b_{ii} + b_{jj} - 2b_{ij}\}_{(ij)\in\Omega}, \sum_j B_{i,j}\Big)$, and write $\tilde{\mathcal{A}}(B) = (\mathcal{P}_\Omega \mathcal{A}(B), \sum_j B_{i,j})$ and $D = \big(\{d_{ij}^2\}_{(ij)\in\Omega}, 0\big)$. By introducing an auxiliary variable $C = B$, we have the following equivalent version

$$\min_{B,C\succeq 0} \mathrm{Tr}(B), \quad \text{s.t.} \quad \mathcal{A}B - D = 0, \quad B = C$$

which can be iteratively solved by

$$\begin{cases} B^{k+1} = \arg\min_B \mathrm{Tr}(B) + \dfrac{\mu_1}{2}\|\mathcal{A}B - D + H_1^k\|_2^2 + \dfrac{\mu_2}{2}\|B - C_k + H_2^k\|_F^2 \\ C^{k+1} = \arg\min_{C\succeq 0} \dfrac{\mu_2}{2}\|B^{k+1} - C + H_2^k\|_F^2, \\ H_1^{k+1} = H_1^k + \mu_1(D - \mathcal{A}B), \\ H_2^{k+1} = H_2^k + \mu_2(C - B), \end{cases}$$

- Convergence of the above algorithm can be theoretically validated as the problem is convex.
- The most time consumption step is to compute the first k eigen-decompositiion with scale $O(n^2k)$

Examples for coordinates reconstruction via matrix completion

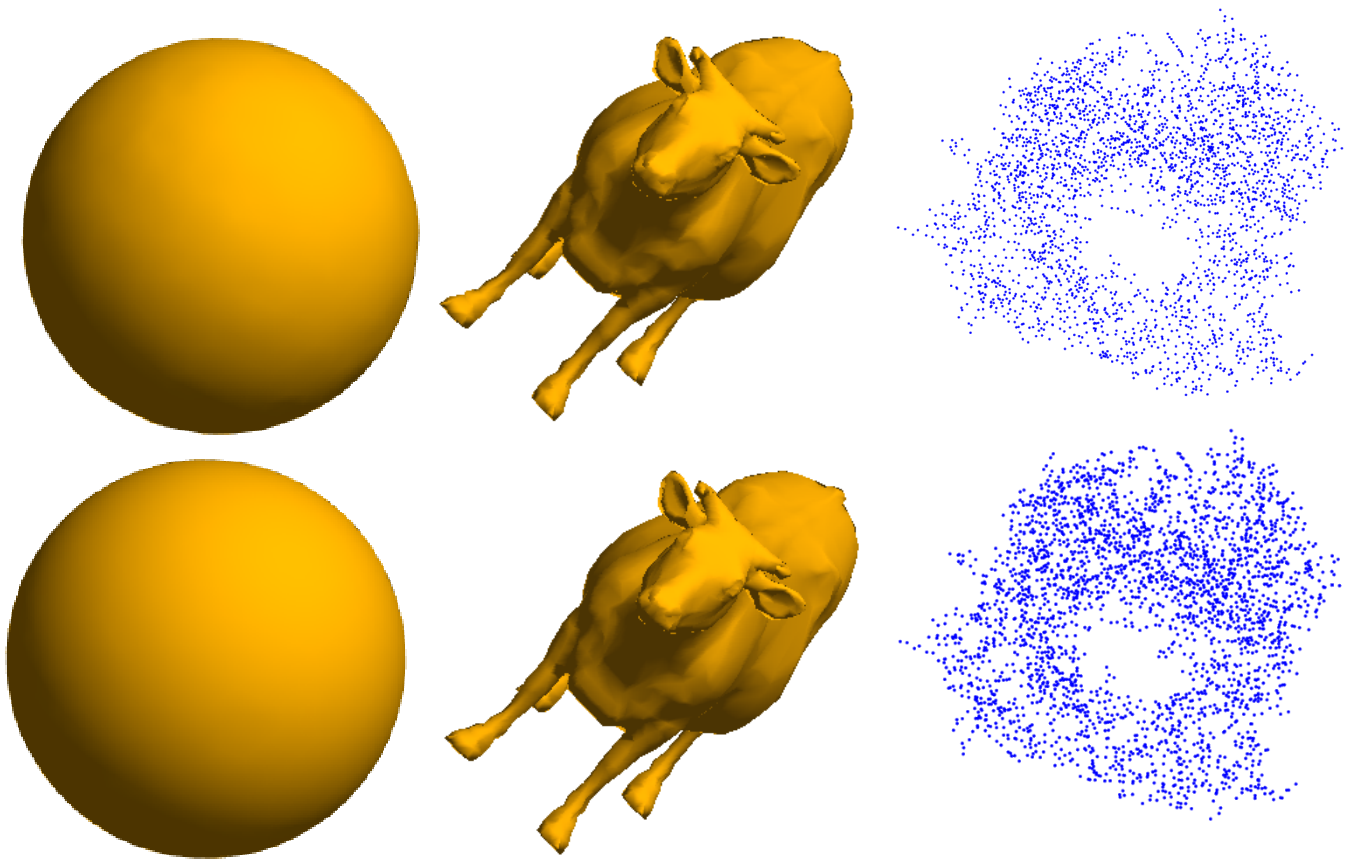

Top:2%, bottom 3%

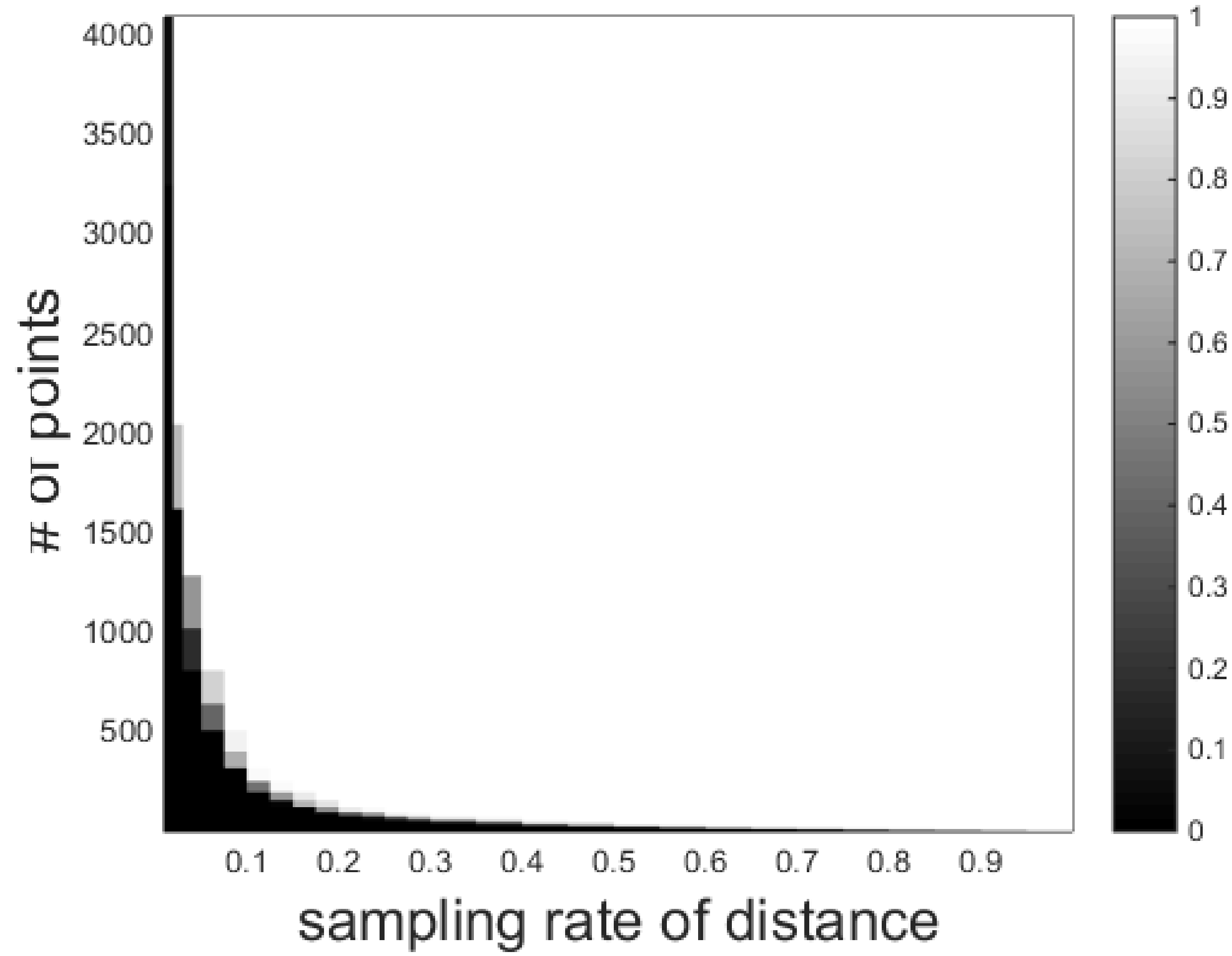

Data \ γ		1%	2%	3%	5%	10%	20%
S^2	E_B	7.157E-1	1.376E-3	4.791E-4	2.474E-4	1.342E-5	4.262E-5
	ρ	0%	92%	100%	100%	100%	100%
Cow	E_B	4.9427E-5	3.980E-4	1.837E-4	5.319E-5	1.4072E-5	2.155E-5
	ρ	100%	100%	100%	100%	100%	100%
Swiss roll	E_B	2.722E-4	2.894E-4	1.633E-4	5.054E-5	1.704E-5	1.114E-5
	ρ	100%	100%	100%	100%	100%	100%

Table 1: Rate of the successful reconstruction ρ and the average relative error E_B out of 50 tests.

Laplace-Beltrami operator: A Bridge from Local to Global

Given a d-dimensional manifold $(\mathcal{M}, g)$,

$$-\triangle_{\mathcal{M}}\phi_n = -\frac{1}{\sqrt{G}}\frac{\partial}{\partial x_i}(\sqrt{G}g^{ij}\frac{\partial \phi}{\partial x_j}) = \lambda_n \phi_n,\ \ n = 0, 1, 2, \cdots$$

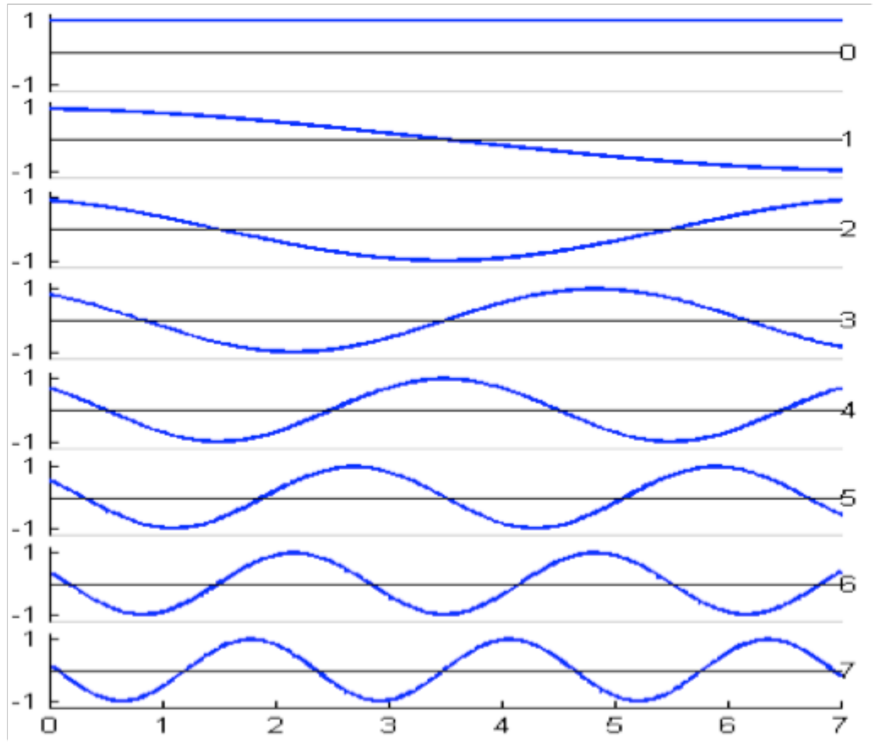

Fourier basis

- Intrinsicness. Invariant under isometric deformation $\mathcal{M}$.
- Inverse spectrum problem.

$$Z(t) = \int_M \sum_i e^{-\lambda_i t}\phi_i(x)\phi_i(y)\mathrm{d}v = \frac{1}{4\pi t}(\sum_{i=0}^{\infty} c_i t^{i/2})$$

where $c_0 = area(M)$, $\quad c_1 = -\frac{\sqrt{\pi}}{2}length(B)$, $\quad c_2 = \frac{1}{3}\int_M K - 1/6\int_B J$.

[McKean-Singer'67]

- Generically, LB eigenfunctions are Morse functions [Uhlenbeck'76].
- LB eigenvalues + LB eigenfunctions uniquely fix a manifold up to isometry. [Perard-Besson-Gassot'94]
- Estimation of LB eigenvalues and the geometry of underlying manifolds.

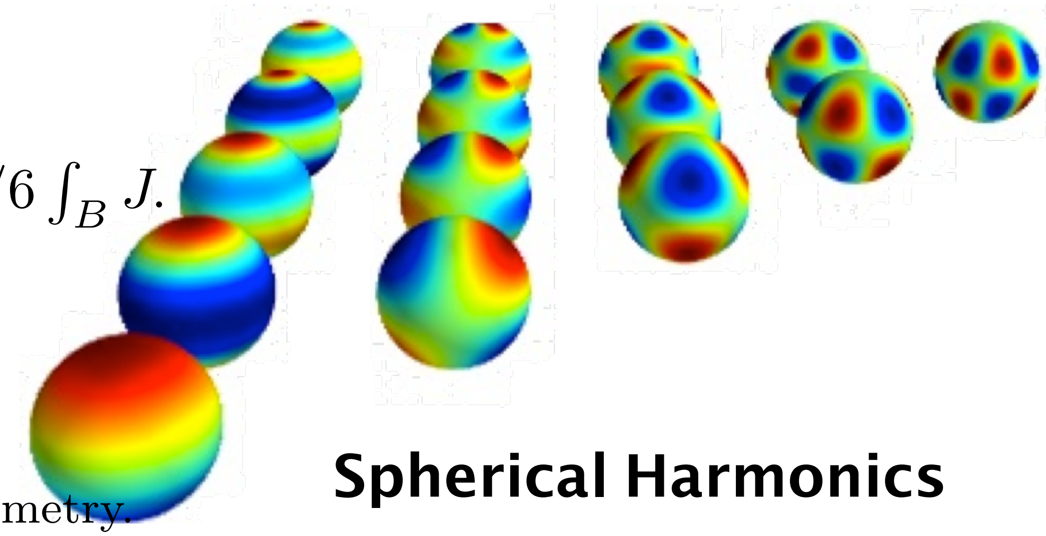

Spherical Harmonics

Local tangent space approximation

- K-nearest neighborhood (KNN)
- Local principle component analysis (PCA)

$$P_i = \sum_{k \in N(i)} (\mathbf{p}_k - \mathbf{c}_i)^T (\mathbf{p}_k - \mathbf{c}_i)$$

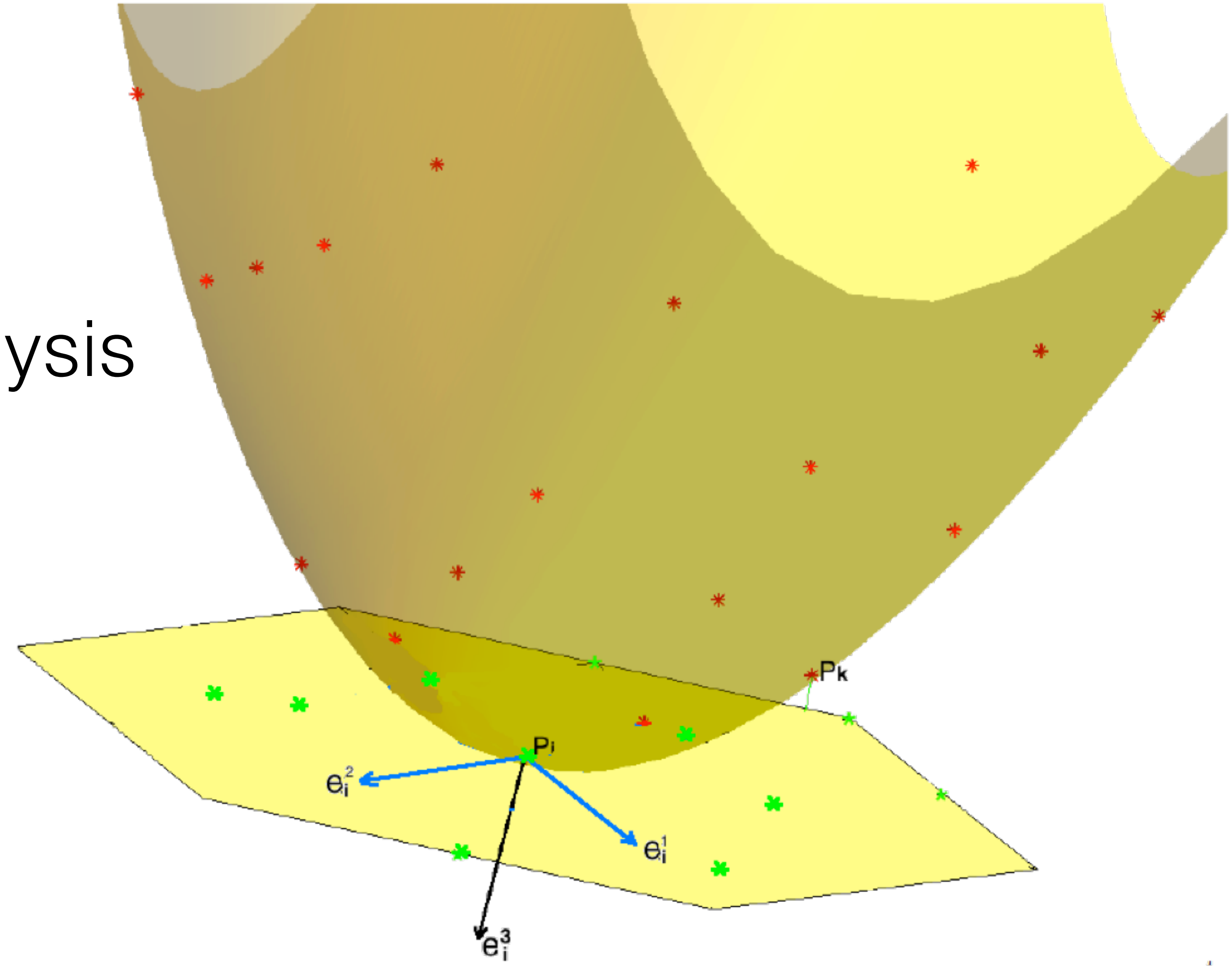

a local coordinate system $\langle \mathbf{p}_i; \mathbf{e}_1^i, \mathbf{e}_2^i, \mathbf{e}_3^i \rangle$ at each point, where eigenvectors $(\mathbf{e}_1^i, \mathbf{e}_2^i, \mathbf{e}_3^i)$ of P_i form an orthogonal frame associated with eigenvalues $(\lambda_1^i, \lambda_2^i, \lambda_3^i)$ with $\lambda_1^i \geq \lambda_2^i \gg \lambda_3^i \geq 0$.

Local manifold approximation using moving least square method

- KNN of $\mathbf{p}_i$ have local coordinates (x_k^i, y_k^i, z_k^i)

- Local manifold approximation. Find a local **degree two bivariate polynomial** $z_i(x, y)$

$$\sum_{k \in N(i)} w(\|\mathbf{p}_k - \mathbf{p}_i\|) \left(z_i(x_k^i, y_k^i) - z_k^i\right)^2 \longrightarrow \Gamma_i = (x, y, z_i(x, y)) \text{ \& Metric } g$$

- Local function approximation. $\displaystyle \min_{f_{\overline{\mathbf{x}}} \in \Pi_m^d} \sum_{k=1}^{K} w(\|\mathbf{x}_k - \overline{\mathbf{x}}\|) \|f_{\overline{\mathbf{x}}}(\mathbf{x}_k) - f_k\|^2$

  where $f_{\overline{\mathbf{x}}}(\mathbf{x}) = \mathbf{b}(\mathbf{x})^T \mathbf{c}(\overline{\mathbf{x}}) = \mathbf{b}(\mathbf{x}) \cdot \mathbf{c}(\overline{\mathbf{x}})$ and $\mathbf{b}(\mathbf{x})$ is the polynomial basis vector.

$$w(d) = \begin{cases} 1 & \text{if } \quad d = 0 \\ 1/k, & \text{if } \quad d \neq 0 \end{cases}, \qquad w(d) = exp(-d^2/\sigma), \qquad w(d) = (1 - \frac{d}{D})^4 (\frac{4d}{D} + 1)$$

Wendland function

- In the local coordinate system, $\mathcal{M}$ and f are well defined function.

$$\nabla_{\mathcal{M}} f = \sum_{i,j=1}^{d} g^{ij} \frac{\partial f}{\partial x_j} \partial_{x_i}, \qquad \mathrm{Div}_{\mathcal{M}} V = \frac{1}{\sqrt{G}} \sum_{i}^{d} \frac{\partial}{\partial x_i} (\sqrt{G} v^i), \qquad \Delta_{\mathcal{M}} \phi = \frac{1}{\sqrt{G}} \sum_{i,j=1}^{d} \frac{\partial}{\partial x_i} (\sqrt{G} g^{ij} \frac{\partial \phi}{\partial x_j})$$

Theorem. *Assume* $f \in C^{m+1}(\mathrm{R}^d)$, $I \leq K$, $w(\cdot) > 0$. *Let* $h = \max_k \ \|\mathbf{x}_k - \overline{\mathbf{x}}\|$ *then*

$$\left| c_i - \frac{1}{\alpha_i!} D^{\alpha_i} f(\overline{\mathbf{x}}) \right| = C h^{m+1-|\alpha_i|}$$

where C *is a constant depends on* w, f *and* α_i. **(Liang-Zhao, natural extension of results in [Levin'98, Lipman et at'06])**

Local Mesh Method [Lai-Liang-Zhao]

1. K nearest neighbor (KNN)

2. Local principal component analysis (PCA) on KNN

$$P_i = \sum_{k \in N(i)} (\mathbf{p}_k - \mathbf{c}_i)^T (\mathbf{p}_k - \mathbf{c}_i)$$

3. Projection on tangent planes.

4. Inherit triangle structure from the tangent space.

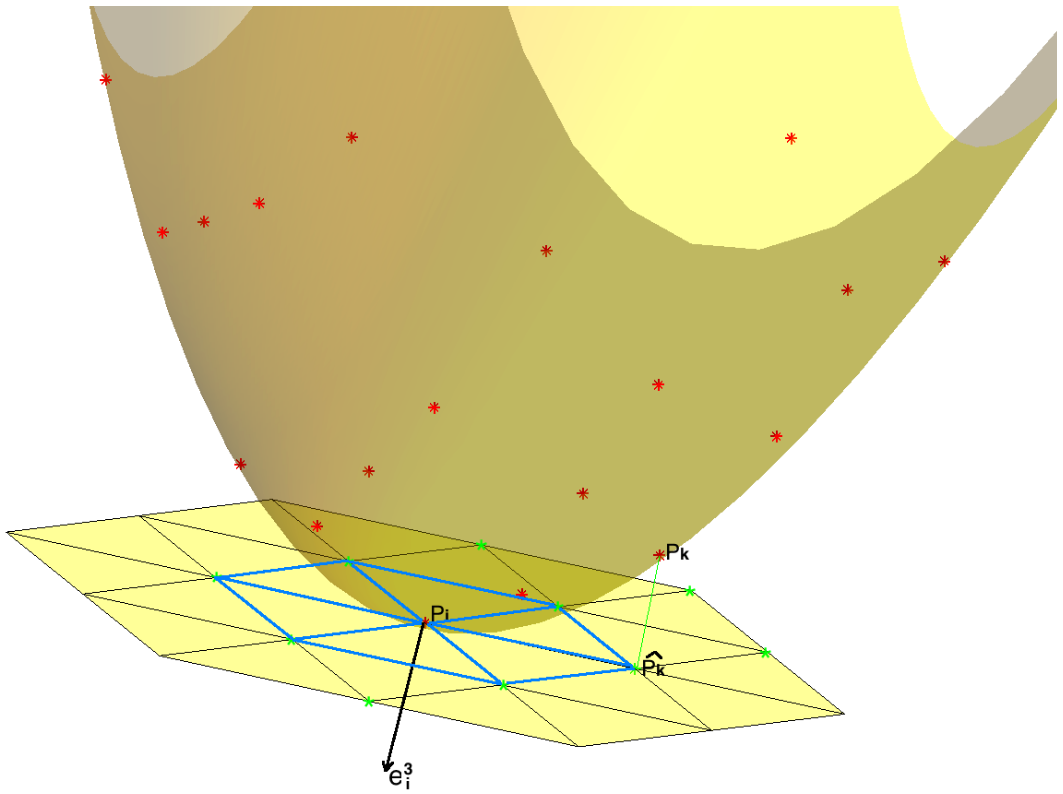

With the local connectivity $\{p_i; \mathcal{V}(i), \mathcal{R}(i)\}$, we have:

$$\nabla_{\mathcal{P}} f(p_i) \approx \frac{1}{W} \sum_{T \in \mathcal{R}(i)} Area(T) \nabla_T f(p_i), \qquad \mathrm{div}_{\mathcal{P}} \overrightarrow{V}(p_i) \approx \frac{1}{W} \sum_{T \in \mathcal{R}(i)} Area(T) \mathrm{div}_T \overrightarrow{V}(p_i)$$

- Only use the first ring structure, more accurate approximation can be obtained using the second ring structure.

- Alternatively, we can also combine the local mesh with the moving least square approximation to obtain better approximation.

Solving PDEs on data represented by incomplete inter-point distance

Key features of our methods:

- No global coordinates or global parameterization is needed.
- Only local information such as K nearest neighbors are needs, which can be reconstructed by matrix completion.
- Our methods works for points sampled from manifolds with representation by incomplete distance. It naturally can work with data in any dimensions and co-dimension.

Solve LB eigenvalue problem based on distance of points on unit sphere

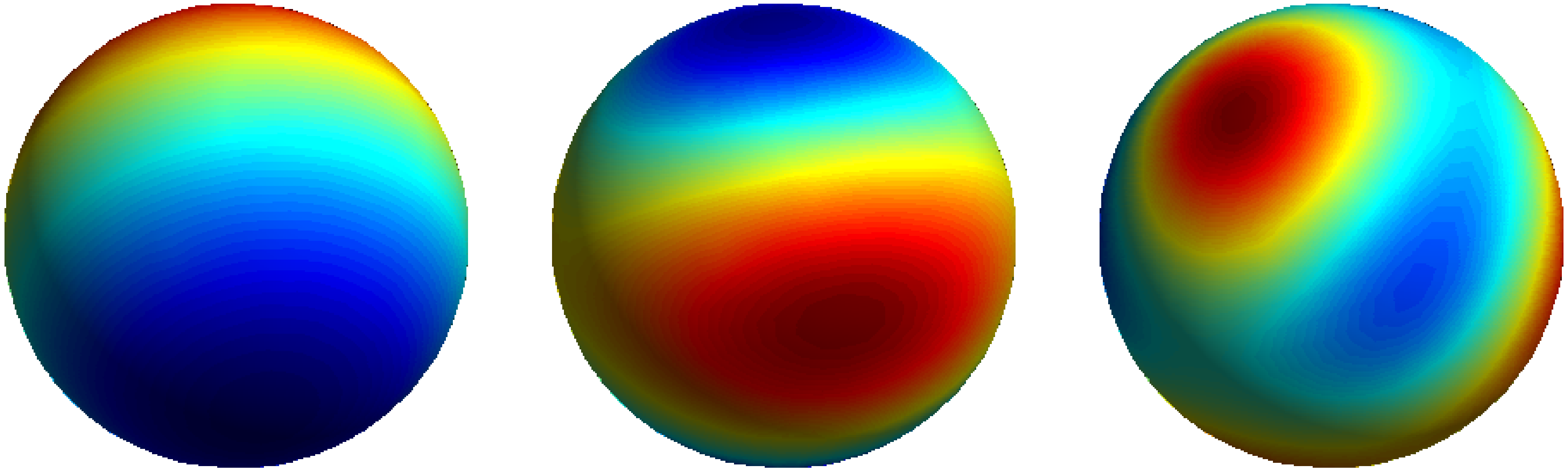

Figure 1: LB eigenfunctions corresponding to $\lambda = 2, 6, 12$ from 80% local distance (1002 points).

sample size	1002	1962	4002	7842	16002
Noise free ($K = 9$)					
$\lambda = 20$	0.0469	0.0280	0.0175	0.0108	0.0046
$\lambda = 72$	0.1292	0.0720	0.0420	0.0256	0.0161
Noise free ($K = 18$)					
$\lambda = 20$	0.0482	0.0250	0.0126	0.0065	0.0032
$\lambda = 72$	0.3643	0.1178	0.0614	0.0328	0.0174
local distance with Gaussian error of $\sigma = 5\% \cdot d_{\max}$ ($K = 18$)					
$\lambda = 20$	0.0469	0.0216	0.0133	0.0081	0.0043
$\lambda = 72$	0.3624	0.1123	0.0625	0.0280	0.0187
Noise free ($K = 30$)					
$\lambda = 20$	0.0850	0.0454	0.0224	0.0115	0.0057
$\lambda = 72$	0.6146	0.3452	0.1041	0.0563	0.0283
local distance with Gaussian error of $\sigma = 10\% \cdot d_{\max}$ ($K = 30$)					
$\lambda = 20$	0.1023	0.0619	0.0393	0.0274	0.0232
$\lambda = 72$	0.6248	0.3653	0.1147	0.0668	0.0395

Table 1: $E_{\max}$ errors for Gaussian perturbed distance of uniformed distributed point clouds of a unit sphere. Assume the inaccurate distance comes from 80% of distance information and corrupted by some type of noise.

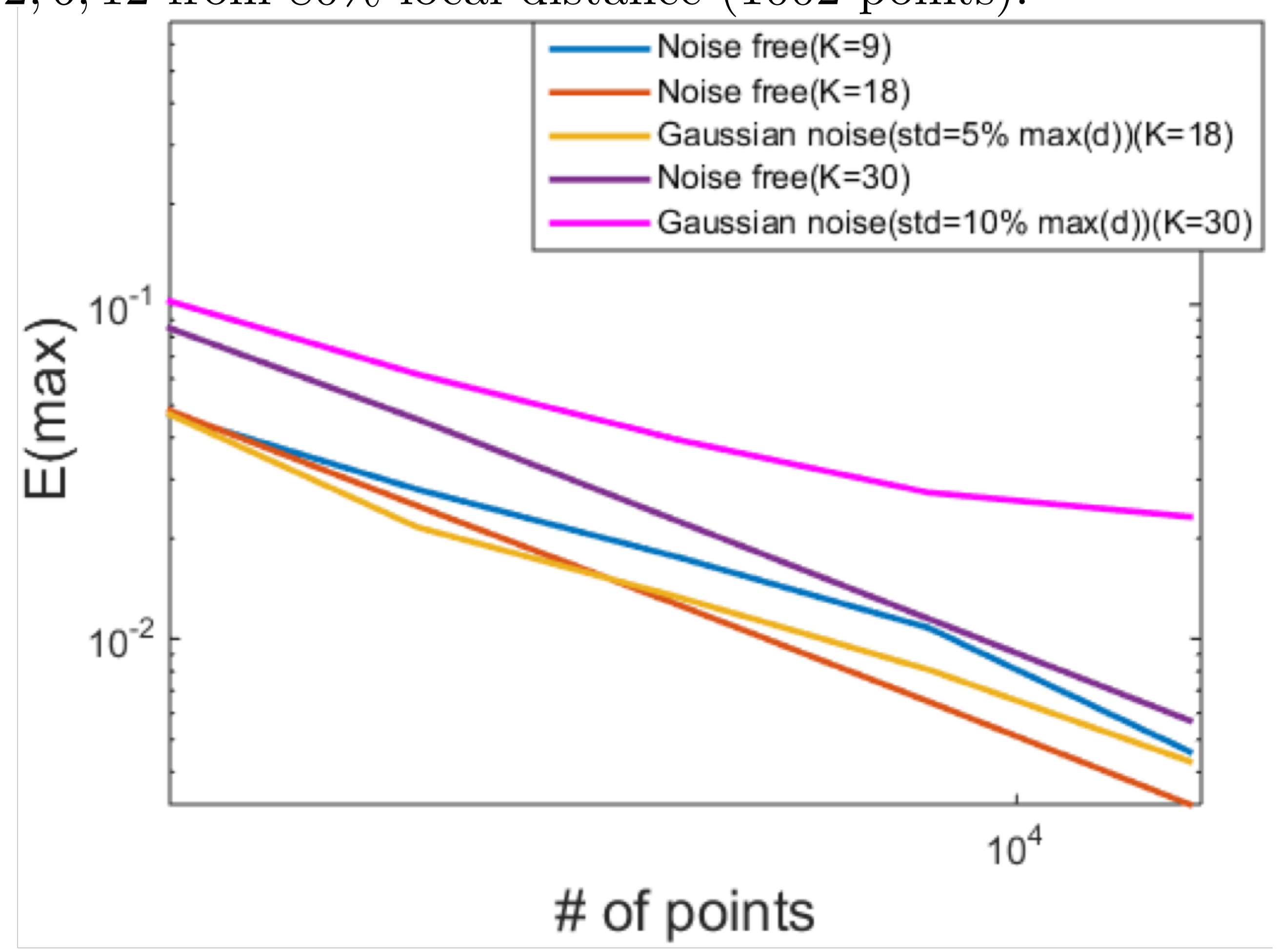

Figure 1: $E_{\max}(\lambda = 72)$ for Gaussian perturbation corrupted distance of uniformed distributed point clouds on the unit sphere.

Local vs. Global: Time consumption comparisons

$$O(n^2m) \text{ vs. } O(nl^2m)$$

number of points				
1002	1962	4002	7842	16002
$\gamma = 100\%$, $\ell = 6$, available distance $= \gamma\ell/n$				
0.26	0.51	1.01	2.03	4.05
$\gamma = 80\%$, $\ell = 9$, available distance $= \gamma\ell/n$				
2.28	5.60	11.17	22.28	45.02
$\gamma = 50\%$, $\ell = 18$, available distance $= \gamma\ell/n$				
4.03	8.09	16.14	32.44	64.71
$\gamma = 30\%$, $\ell = 30$, available distance $= \gamma\ell/n$				
15.13	30.19	60.42	120.95	241.63
global reconstruction using 3% distance ($\ell = 6$ for MLS)				
2.09	9.86	40.13	154.40	597.06

Table 1: Comparisons of time consumption (minutes) of solving the LB eigenvalue problem based on local/global reconstruction methods.

Solve LB eigenvalues for distance data from high-D manifolds

LB eigenkproblem for a 2 dimensional flat torus in $\mathbb{R}^4$.

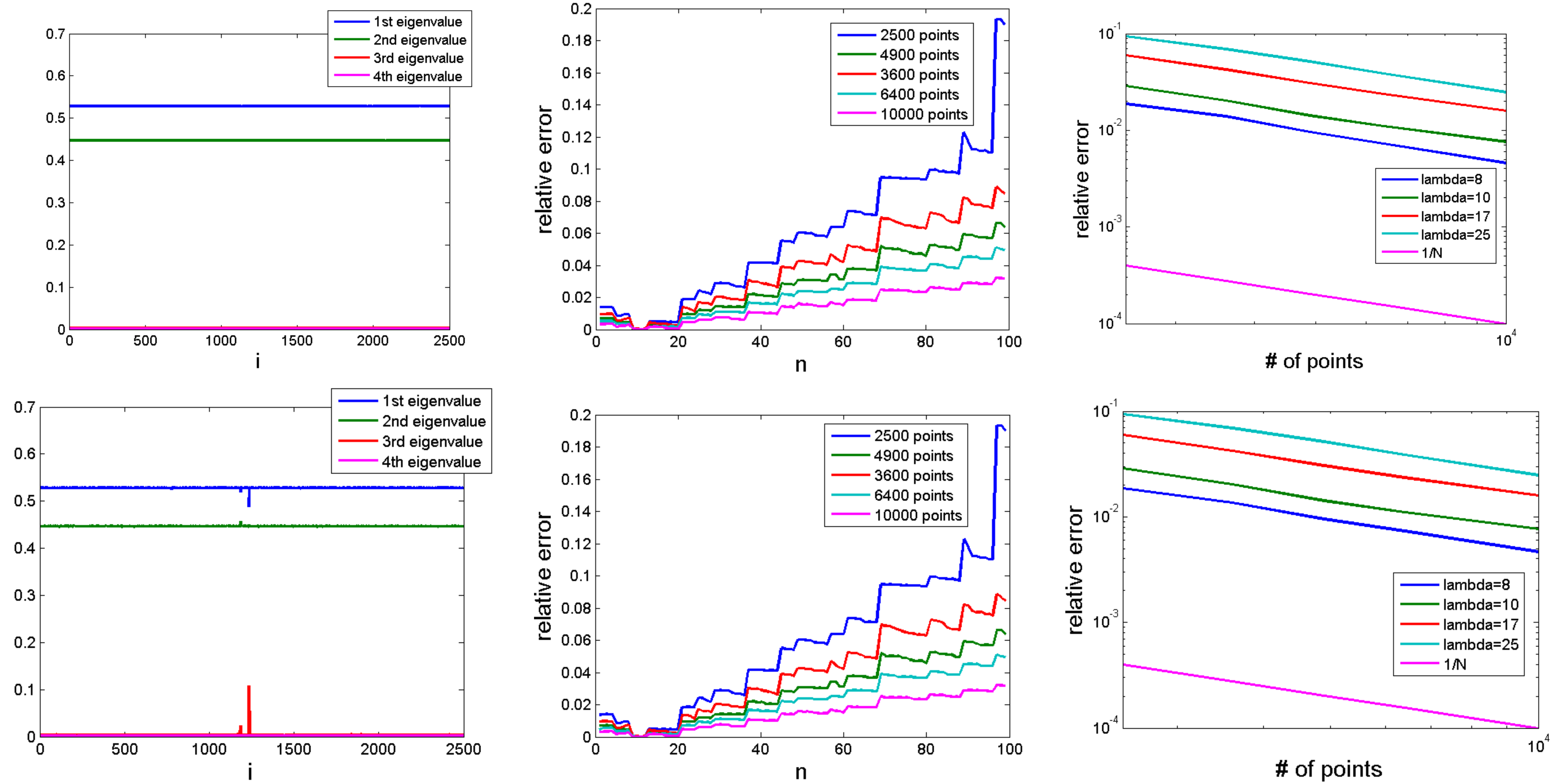

Figure 1: a 2D torus $\mathbb{R}^4$ with 2500 points. Bottom: Relative errors. Top: full distance. Bottom: 60% distance. Left: The largest 4 eigenvalues of inner-product matrix. Middle: Relative error for the fist 100 eigenvalues. Right: Convergence curves.

Solve LB eigenvalues for distance data from high-D manifolds

LB eigenkproblem for a 3 dimensional flat torus in $\mathbb{R}^6$.

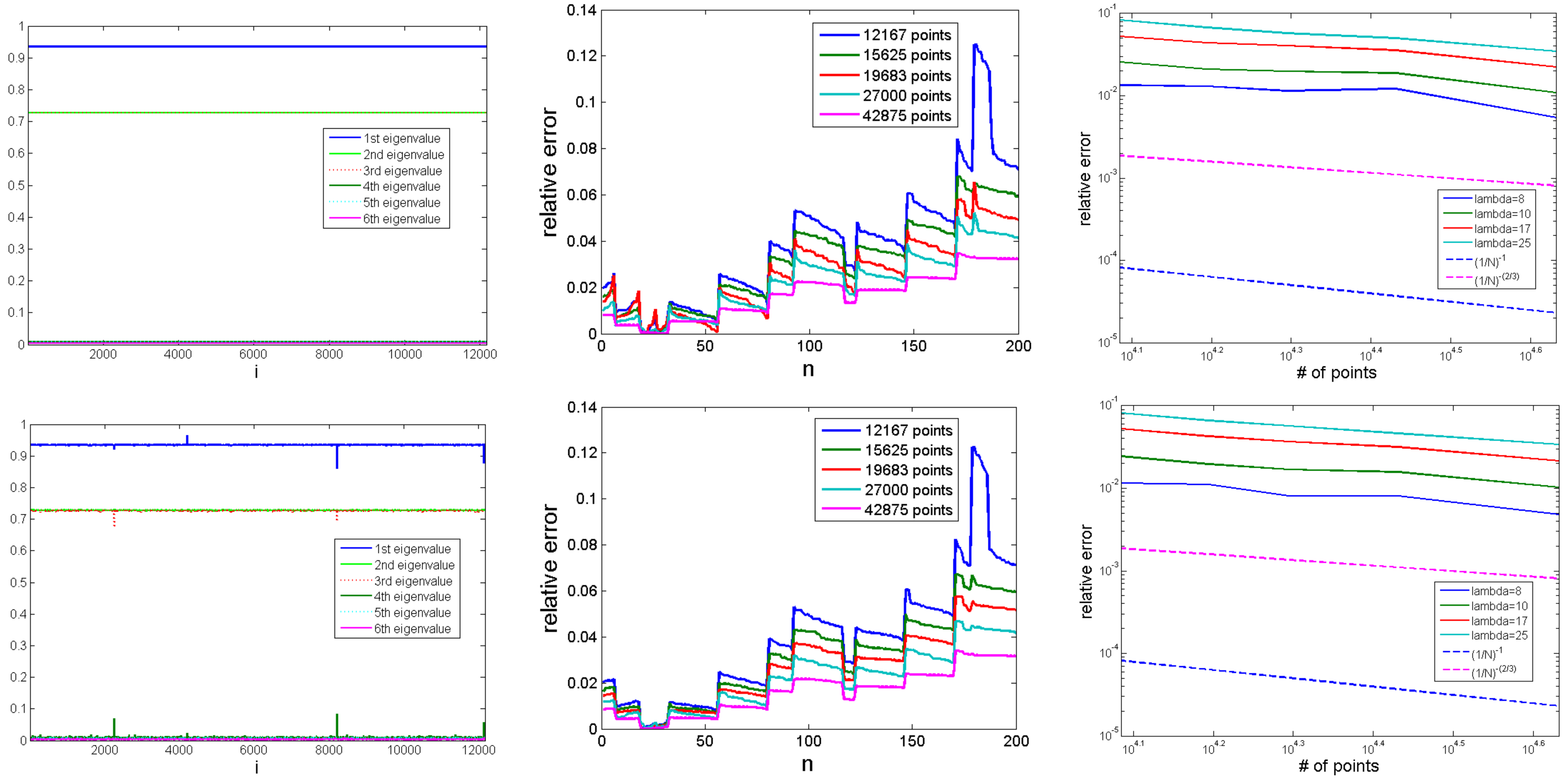

Figure 1: a 3D torus $\mathbb{R}^6$ with 12167 points. Bottom: Relative errors. Top: full distance. Bottom: 60% distance. Left: The largest 4 eigenvalues of inner-product matrix. Middle: Relative error for the fist 100 eigenvalues. Right: Convergence curves.

More examples for solving LB eigenvalue problem

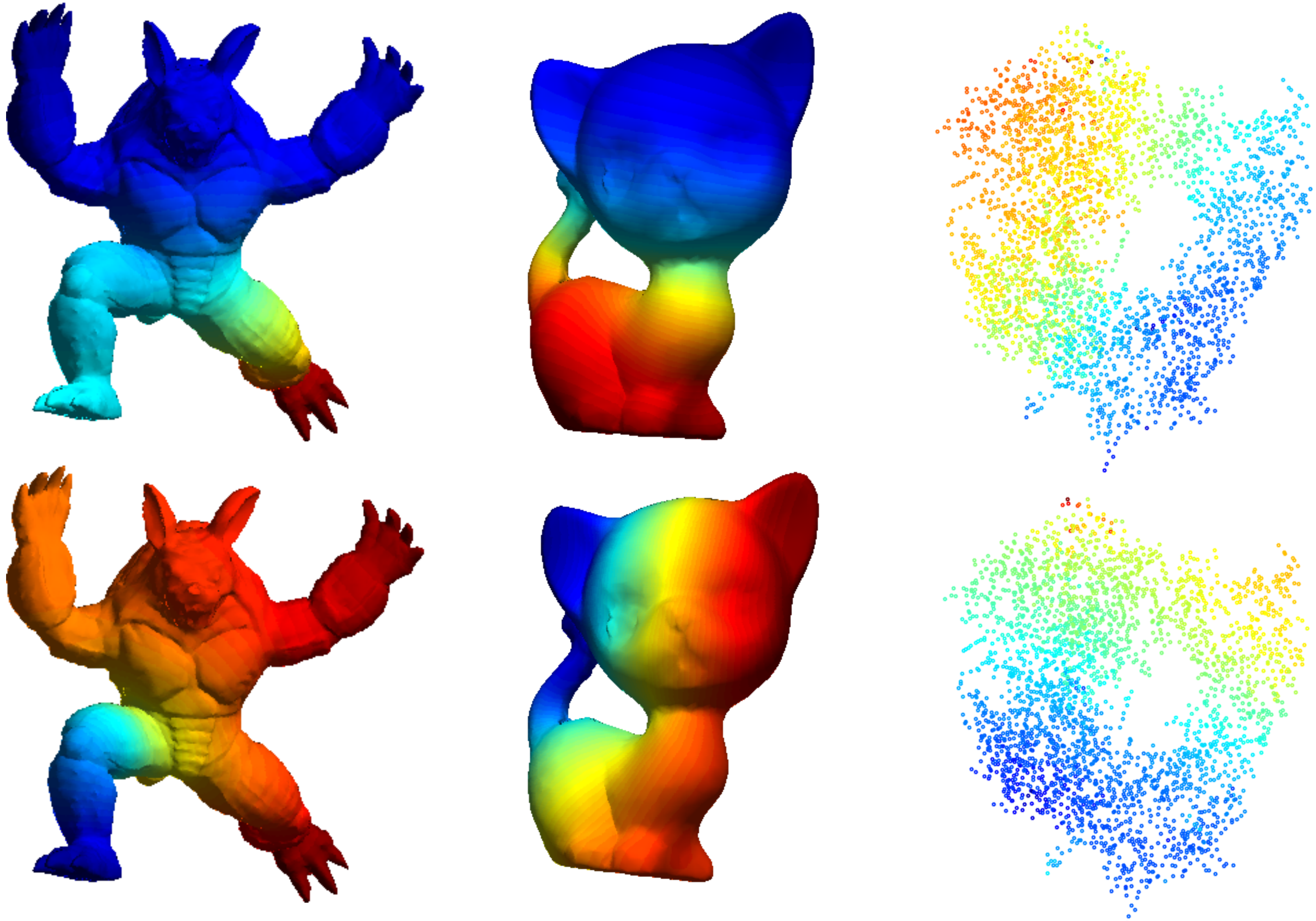

1st and 2nd LB eigenvalues based on 50% local distance matrix.
(For the first 2, mesh is only used for visualization)

A non diffusion type: Eikonal equation from distance

The Eikonal equation for the distance map on $\mathcal{M}$:

$$\begin{cases} |\nabla_{\mathcal{M}} d(x)| = 1 \\ d(x) = 0, \quad x \in \Gamma \subset \mathcal{M} \end{cases}$$

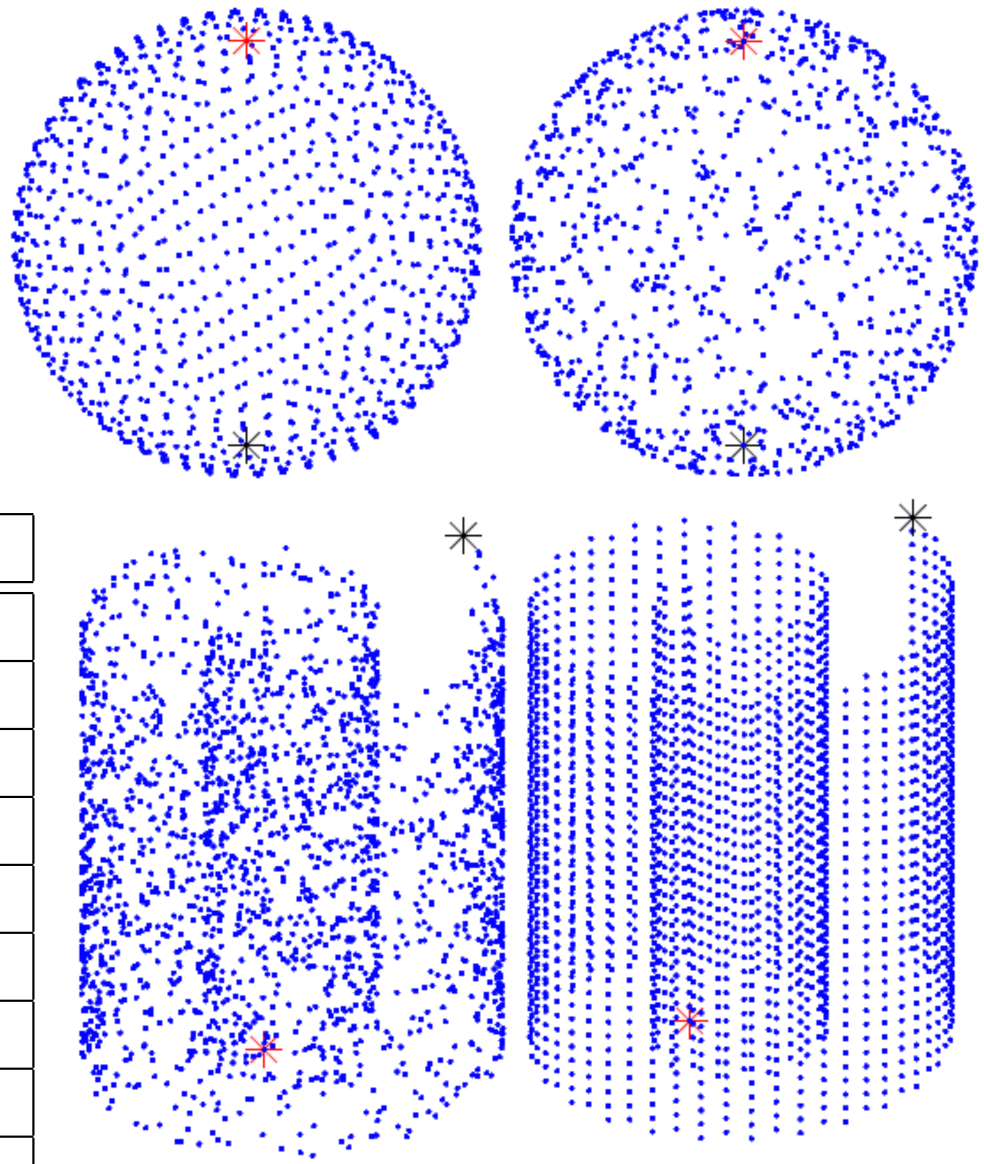

Uniform sampling on S^2					
sample size	1002	1962	4002	7842	16002
Dijkstra	0.008615	0.008606	0.008296	0.010642	0.011501
our method	0.008100	0.005890	0.004110	0.002877	0.002158
Non-uniform sampling on S^2					
Dijkstra	0.011209	0.016090	0.018380	0.016391	0.019953
our method	0.012016	0.008792	0.003742	0.001736	0.002765
Uniform sampling on swiss roll					
Dijkstra	0.013104	0.021242	0.024560	0.024311	0.026004
our method	0.003127	0.001637	0.001130	0.000783	0.000620
Non-Uniform sampling on swiss roll					
Dijkstra	0.016612	0.015779	0.014573	0.016587	0.018649
our method	0.004754	0.005189	0.003087	0.005171	0.007246

Table 1: Relative error of geodesic distances from north pole to south pole reconstructed from 60% of local distances in each point's 20 nearest neighbourhoods.

Construction of Skeleton

Reeb graph and skeleton structure obtained from LB eigenfunction ϕ:

Quotient space: $\mathcal{M}/\sim$: $x \sim y \iff \phi(x) = \phi(y)$. This can be used to medical image analysis and data analysis

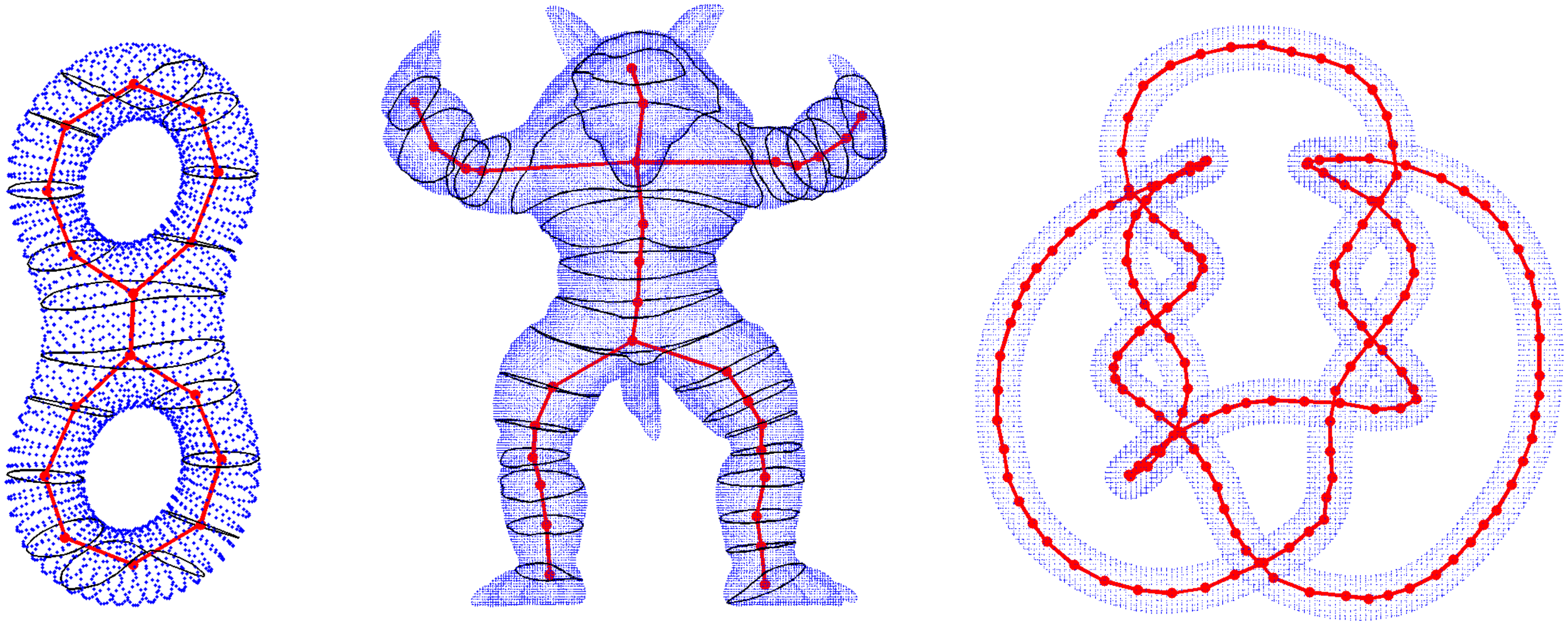

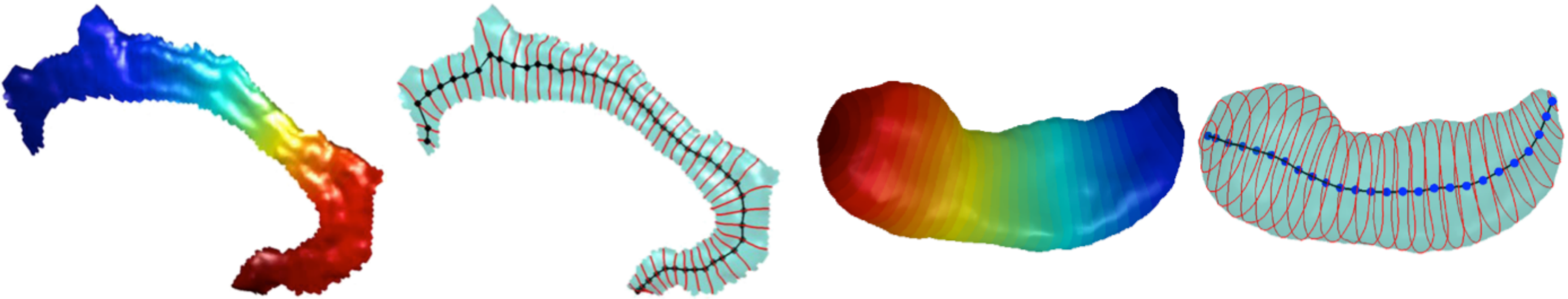

Shape DNA [Reuter'06]

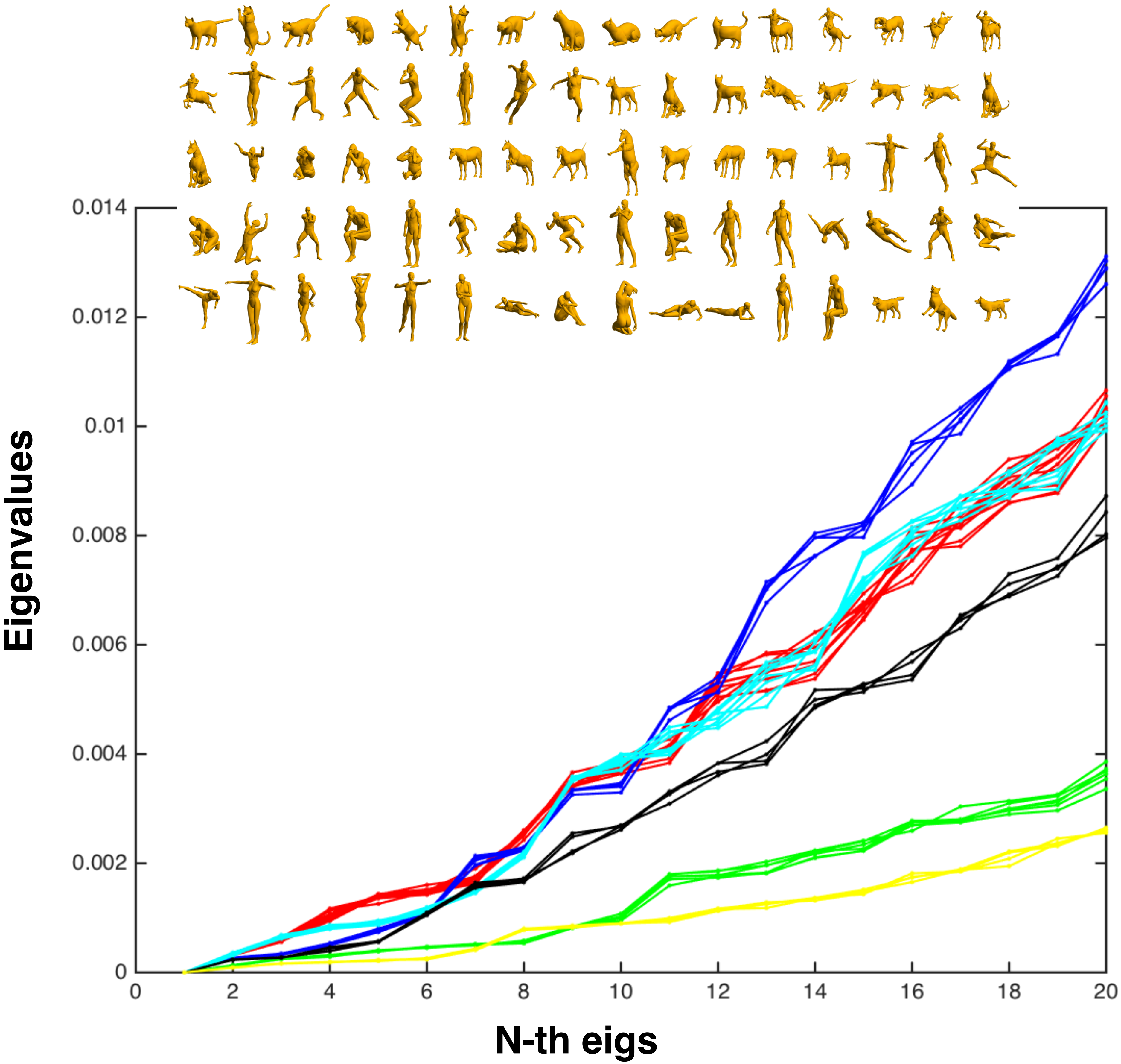

Intrinsic comparisons using LB eigenmaps + optimal transportation [Lai-Zhao'16]

Rotation-Invariant sliced-Wasserstein distance for registration:

$$\mathrm{RSWD}\Big((\mathcal{P},\mu^{\mathcal{P}}),(\mathcal{Q},\mu^{\mathcal{Q}})\Big)^2 = \min_{R\in O(n)} \int_{S^{n-1}} \min_{\sigma\in \mathrm{ADM}(\pi_{\#}^{\theta,R}\mu^{\mathcal{P}},\pi_{\#}^{\theta}\mu^{\mathcal{Q}})} \int_{\mathbb{R}\times\mathbb{R}} \|x-y\|_2^2 \,\mathrm{d}\sigma(x,y)\ \ \mathrm{d}\theta$$

Theorem (Lai-Zhao)**.** RSWD$(\cdot,\cdot)$ *defines a distance on the space* $\mathfrak{M}_n/\sim$.

David2 to David1

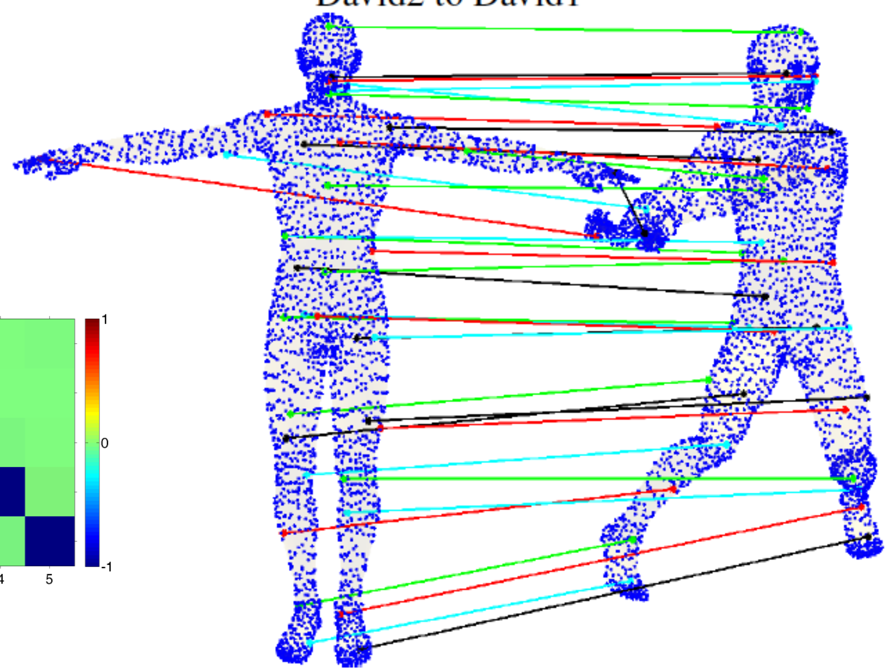

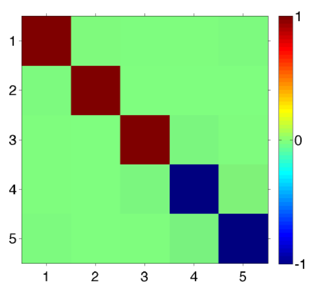

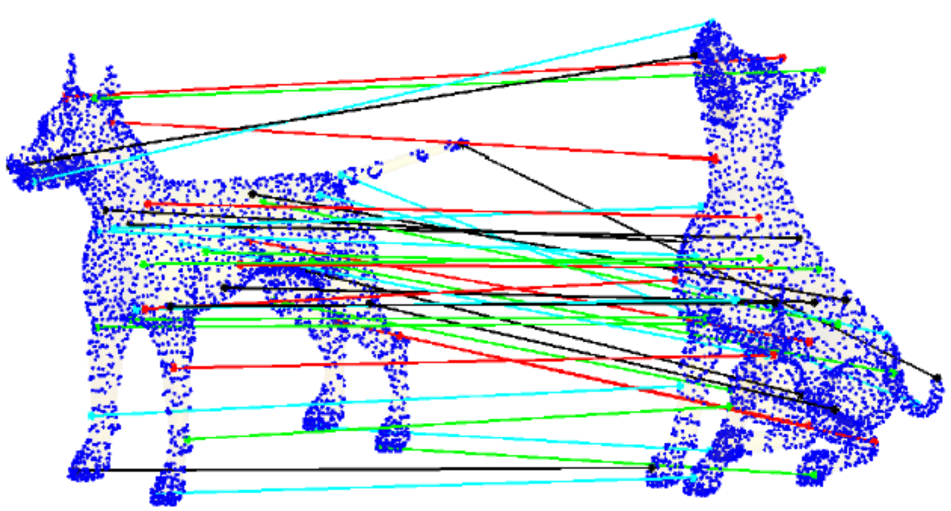

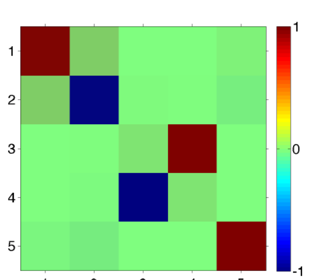

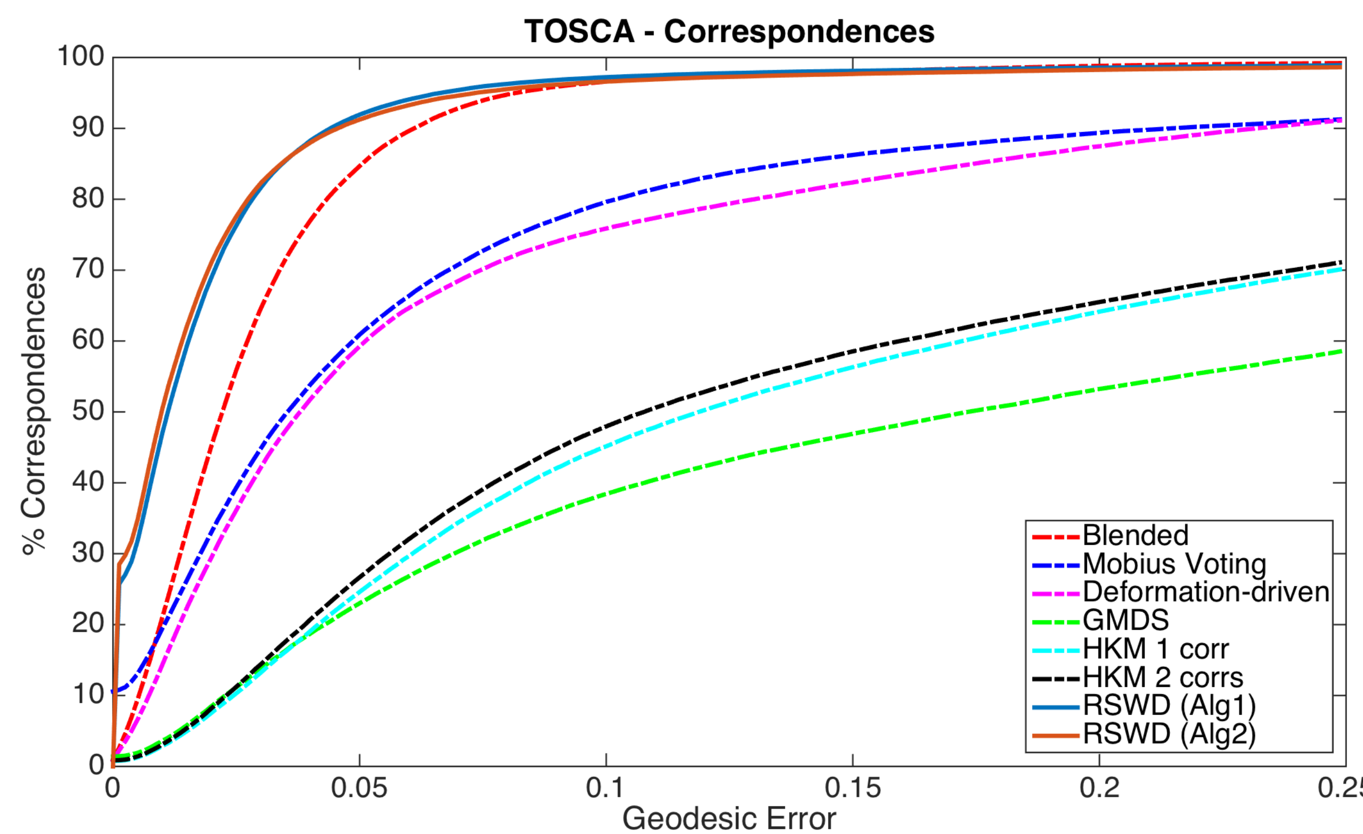

Manifold stitching from distance

- $P \approx \sum_{i=1}^{N} \phi_i \alpha_i \longleftrightarrow \min_{\alpha} \|P - \Phi\boldsymbol{\alpha}\|_F^2$. The coefficients $\boldsymbol{\alpha}$ do not depend on location.

- Stitching patches using LB eigenfunctions

$$\min_{\boldsymbol{\alpha},\{R_j\},\{b_j\}} \sum_{j=1}^{N_p} \|Q_j - \Phi_j \boldsymbol{\alpha} R_j - \mathbf{1} b_j\|_F^2, \quad \text{s.t.} \quad R_j^\top R_j = I_d$$

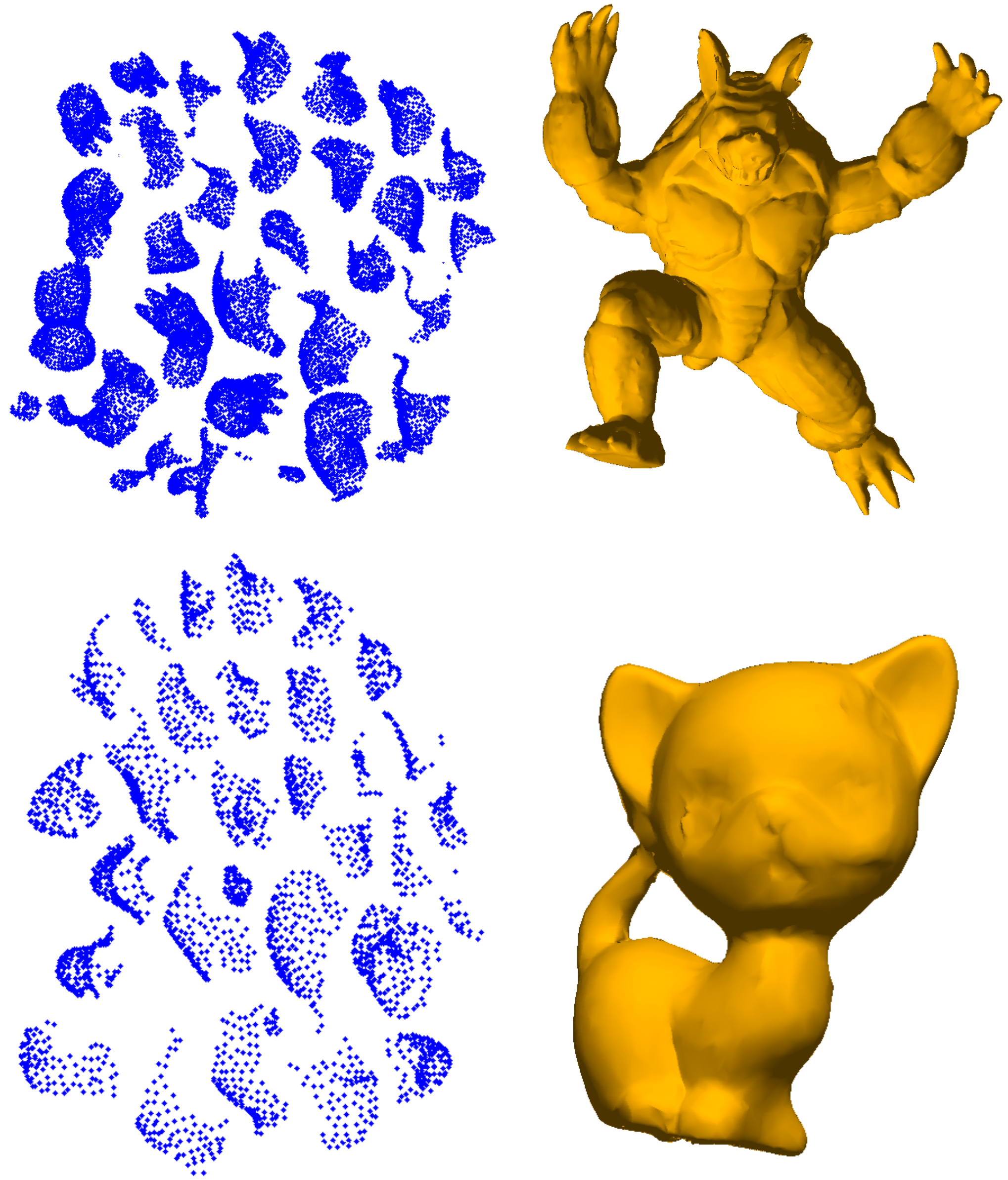

Figure 1: 50% of local Euclidean distance. Armadillo (16519 points), Kitten (2884 points)

data / methods	Armadillo	Kitten	Swiss roll
Global recon	35321.84	1315.50	622.65
Stitching	760.18	138.76	199.75

Computation

Dimension reduction using geodesic distance

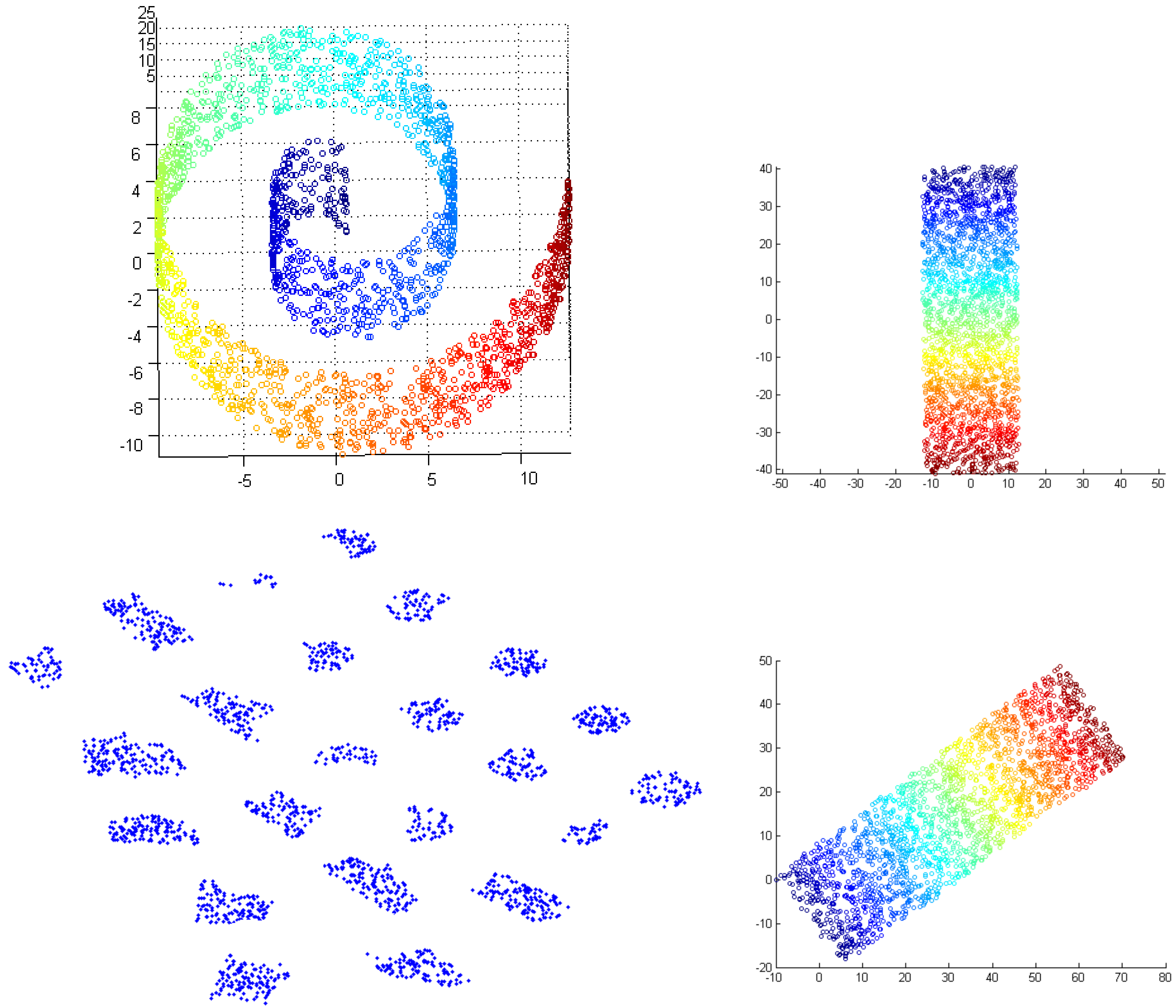

Figure 1: Top: the swiss roll surface (left) and its dimensional reduction result (right) from randomly 3% of pair-wise geodesic distance. Bottom: local and global coordinates reconstruction of the swiss roll from its 80% local geodesic distance.

Some extensions to other problems

Extension to Manifold low-rank for EDG

$$\min_P \sum_i \operatorname{rank}(R_{\Omega_i}(P)), \quad \text{s.t.} \mathscr{A}(PP^\top) = D.$$

$$\min_P \sum_i \|R_{\Omega_i}(P)\|_*, \quad \text{s.t.} \mathscr{A}(PP^\top) = D.$$

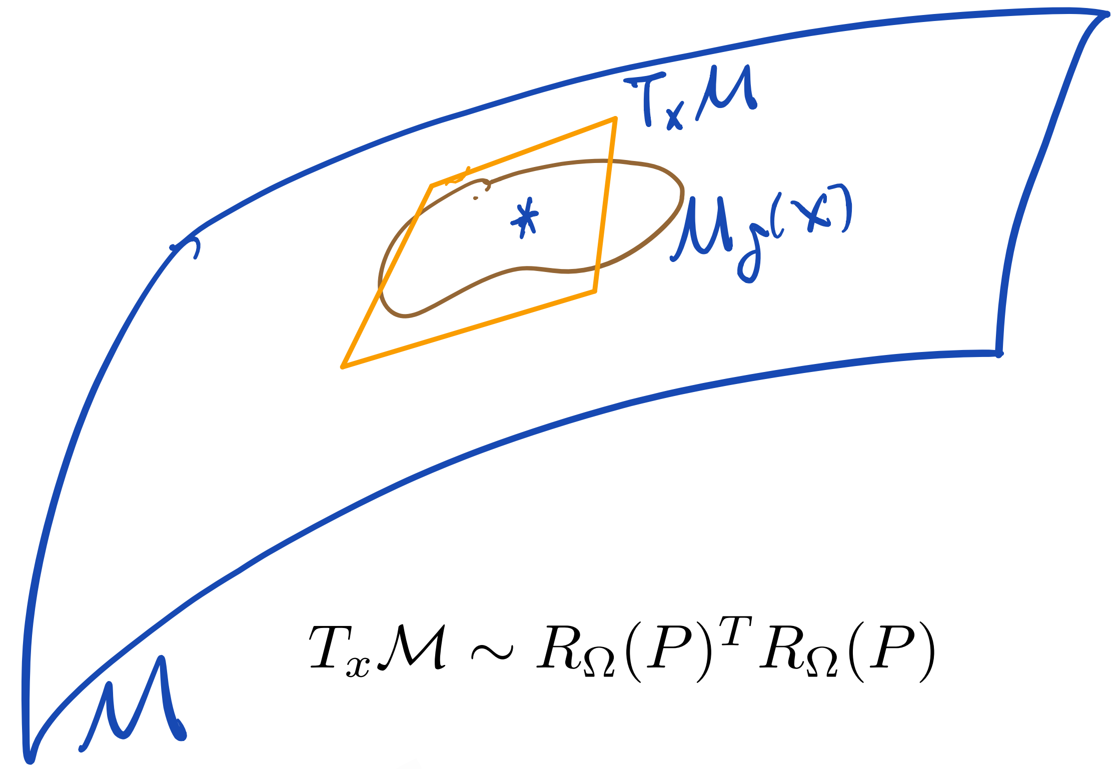

$$T_x\mathcal{M} \sim R_\Omega(P)^T R_\Omega(P)$$

5%

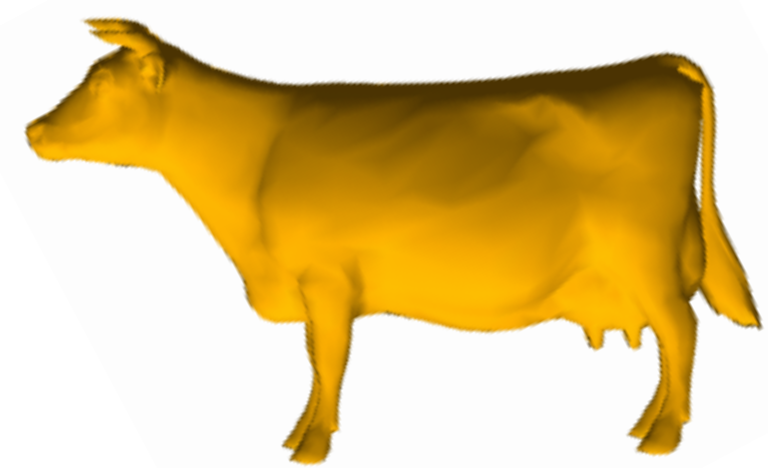

5%

Semi-supervised learning

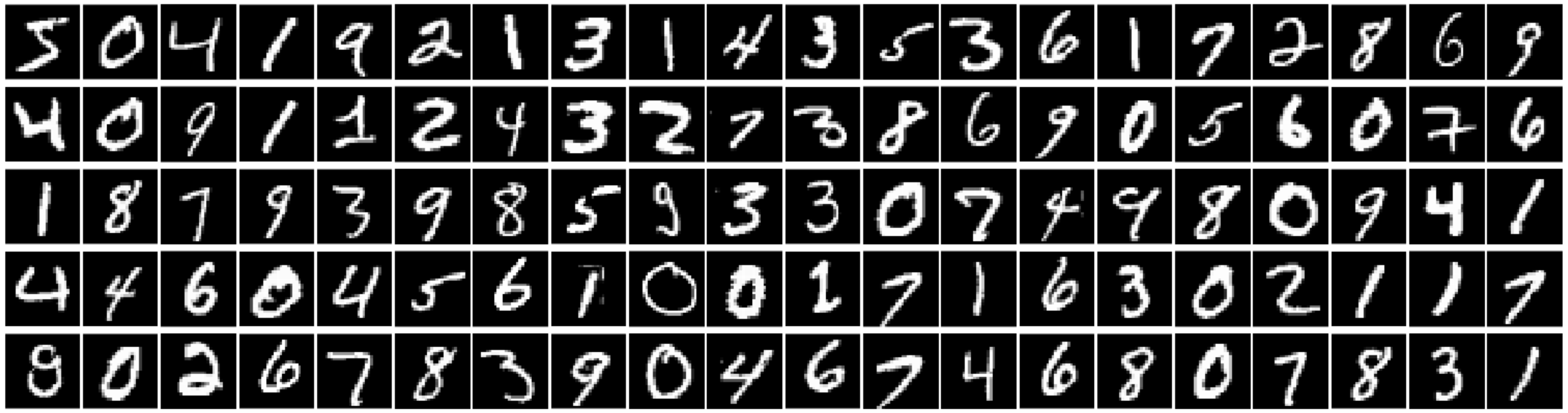

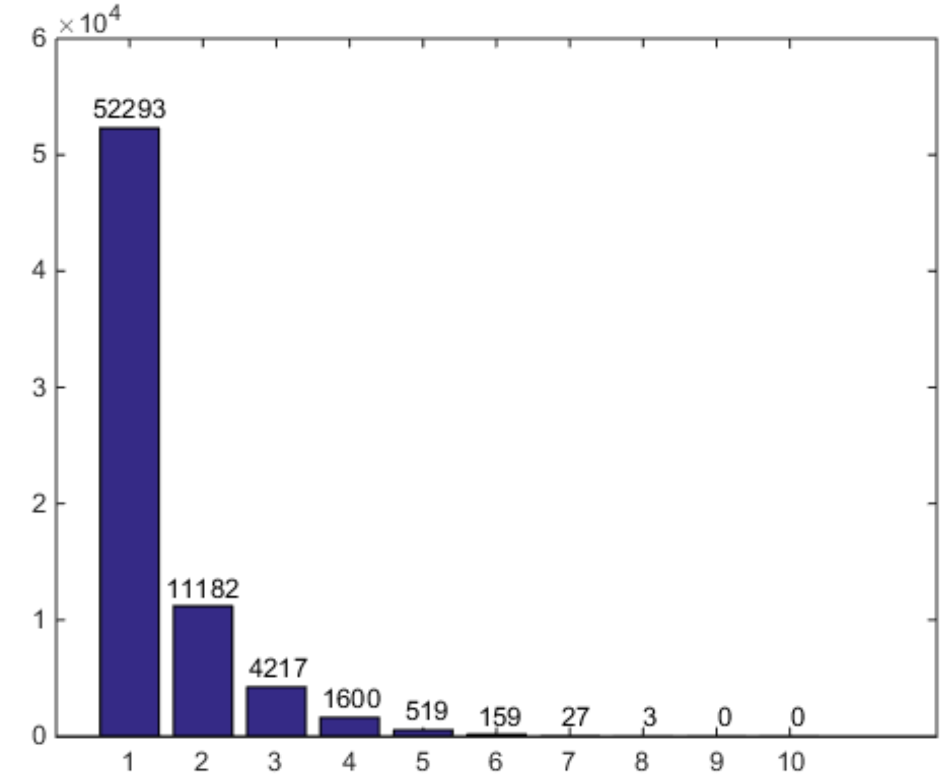

Rank histogram

we define the cluster functions $\{\phi_i(x)\}$ which is partially assigned from the training data S.

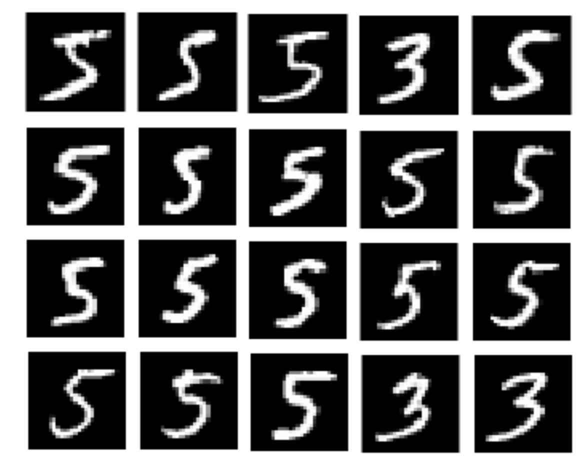

a rank-2 patch

$$\phi_i(x) = \begin{cases} 1, & L(x) = i. \\ 0, & \text{otherwise.} \end{cases} \quad , x \in S, \quad i = 0, 1, 2, \ldots, l.$$

$$\min_{\Phi} \sum_{x \in \mathscr{I}} \|(R_{\mathcal{M},x})\Phi\|_*, \quad \text{s.t.} \quad P \subset \mathcal{M}, \quad \Phi(x,i)|_{x\in S} = \begin{cases} 1, & L(x) = i. \\ 0, & \text{otherwise.} \end{cases}$$

Semi-supervised learning: MINST, 70K images

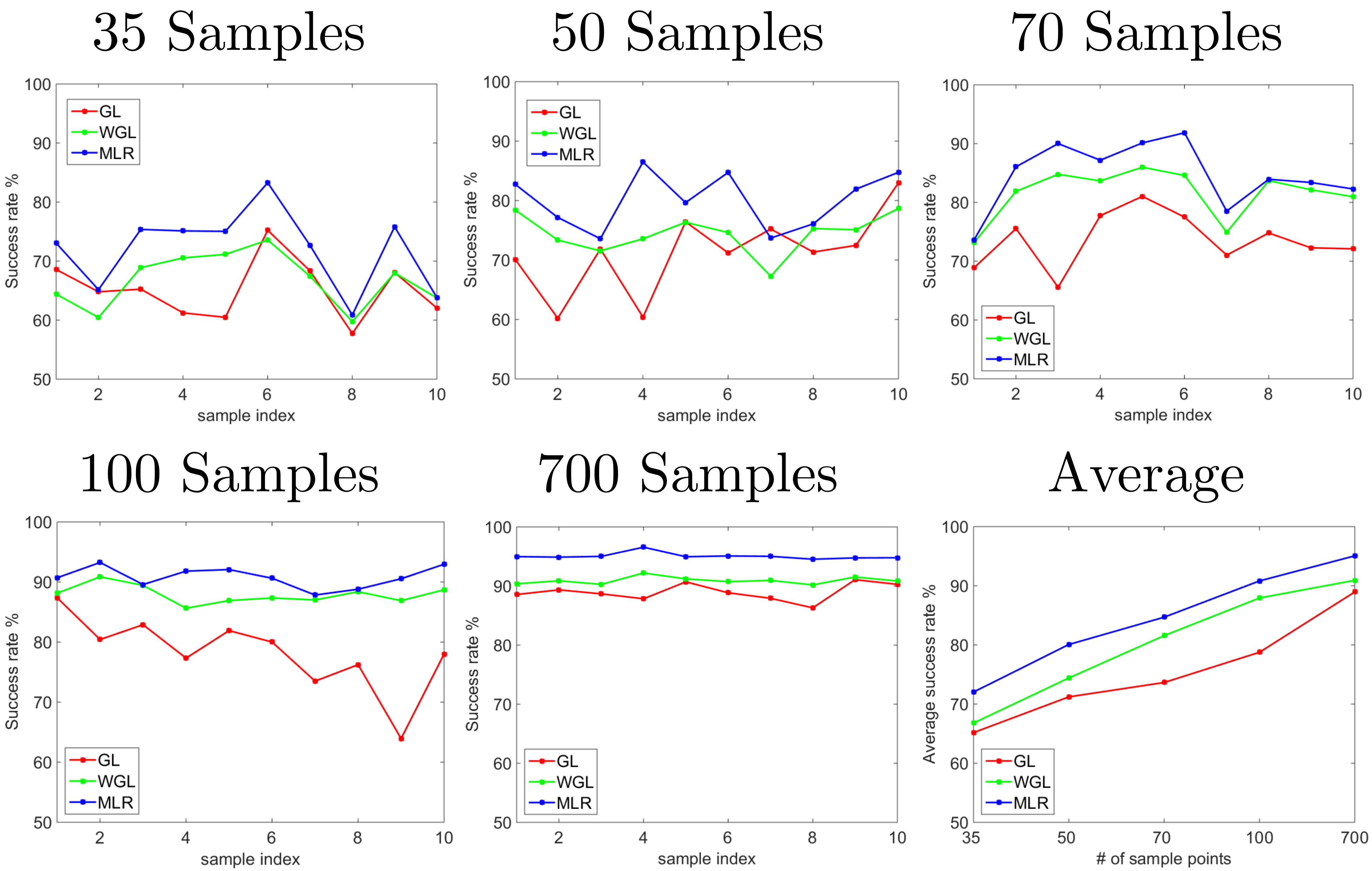

Figure 1: Success rate of label estimation by graph Laplacian, weighted graph Laplacian, and proposed MLR methods.

Extension to Image Processing: Patch Manifold and LDMM [Osher-Shi-Zhu'16]

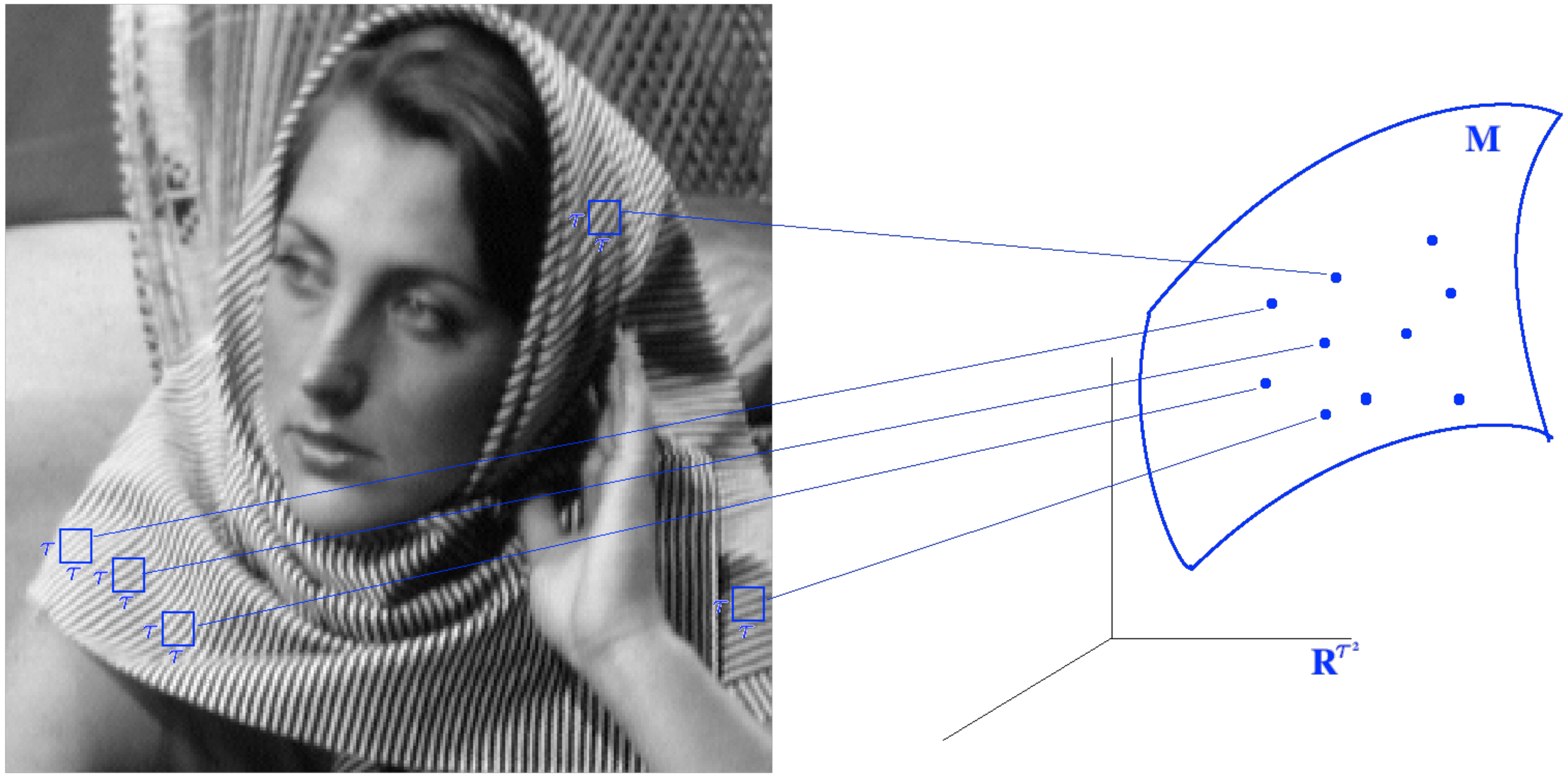

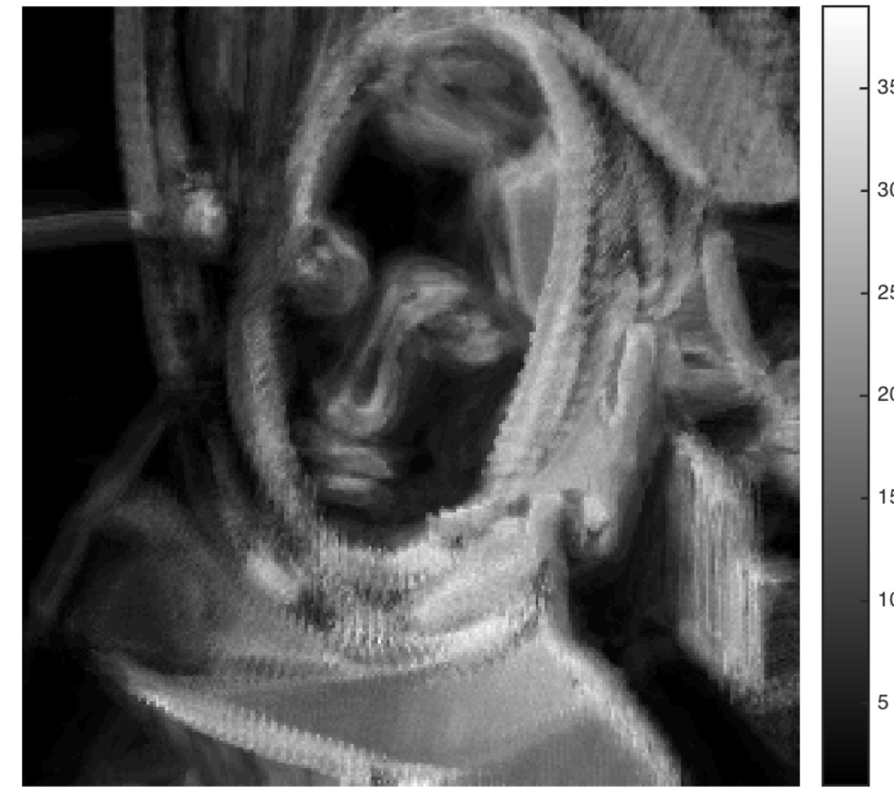

$$\min_{f} dim(\mathcal{M}(f)) + \frac{\mu}{2}\|Af - f_0\|^2$$

$$\min_{f\in\mathbb{R}^{m\times n}, D, \mathcal{M}\subset R^d} \frac{1}{2}\sum_{i=1}^{d}\int_{\mathcal{M}} |\nabla_{\mathcal{M}} a_i(p)|^2 \, \mathrm{d}\mathcal{M} + \frac{\mu}{2}\|Af - f_0\|^2, \quad \text{s.t.} \quad \mathcal{P}(f)\subset\mathcal{M}$$

A Patch manifold based low-rank regularization model [Lai-Li'17]

$$\min_{\mathcal{M}\subset\mathbb{R}^{\tau^2},f} \sum_{x\in\mathscr{I}} \mathrm{rank}((R_{\mathcal{M},x})(\mathcal{P}(f)), \quad \text{s.t.} \quad \mathcal{P}(f)\subset\mathcal{M}, \quad \mathcal{A}f = g.$$

Inspired by matrix completion theory, we use nuclear norm to approximate rank which provides:

$$\min_{\mathcal{M}\subset\mathbb{R}^{\tau^2},f} \sum_{x\in\mathscr{I}} \|(R_{\mathcal{M},x})(\mathcal{P}(f))\|_* \qquad \text{s.t.} \quad \mathcal{P}(f)\subset\mathcal{M}, \quad \mathcal{A}f = g.$$

with diffusion:

$$\min_{\mathcal{M}\subset\mathcal{R}^{\tau^2},f} \sum_{x\in\mathscr{I}} \|R_{\mathcal{M},x}(\mathcal{P}(f))\|_* + \frac{\lambda}{2}\|\nabla_{\mathcal{M}} f\|_2^2, \quad \text{s.t.} \quad \mathcal{P}(f)\subset\mathcal{M}, \quad \mathcal{D}(f) = g,$$

- **Need to update manifold and f both;**
- **It is a non-convex problem;**
- **For each point, SVD is only applied to a small size matrix;**

Example: Image inpainting

Ground Truth | Incomp. image (5.90 dB) | Harmonic Ext. (22.46 dB) | Wavelet (22.83 dB)

TV (21.97 dB) | LDMM (23.73 dB) | LDMM+WGL (25.84 dB) | **MLR** ($\lambda = -20$, 26.09 dB)

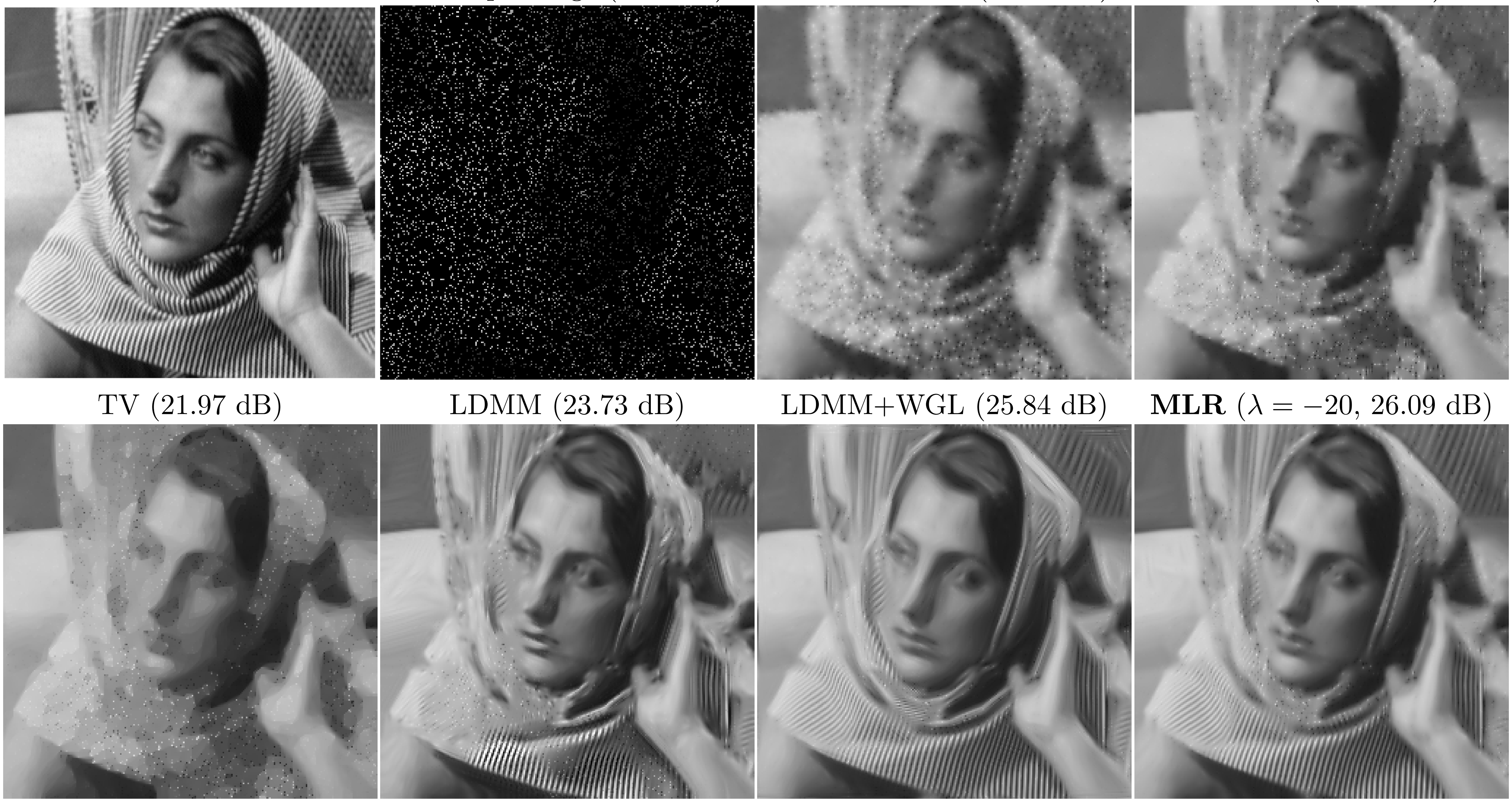

Figure 1: Image inpainting results of 256×256 Barbara image from 10% random available pixels using different methods

Image inpainting

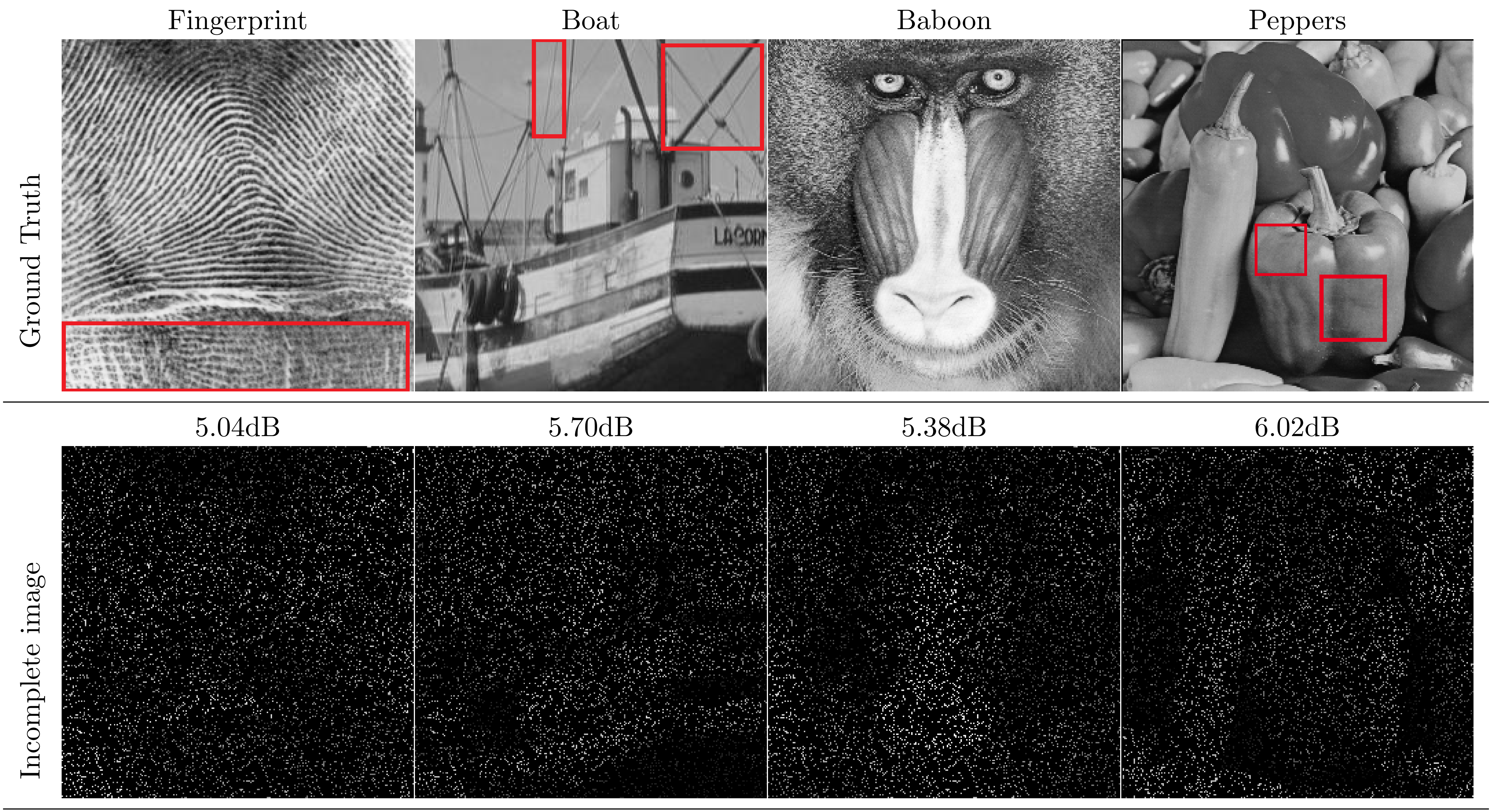

Figure 1: Image inpainting for different images from 10% available pixels.

Image inpainting

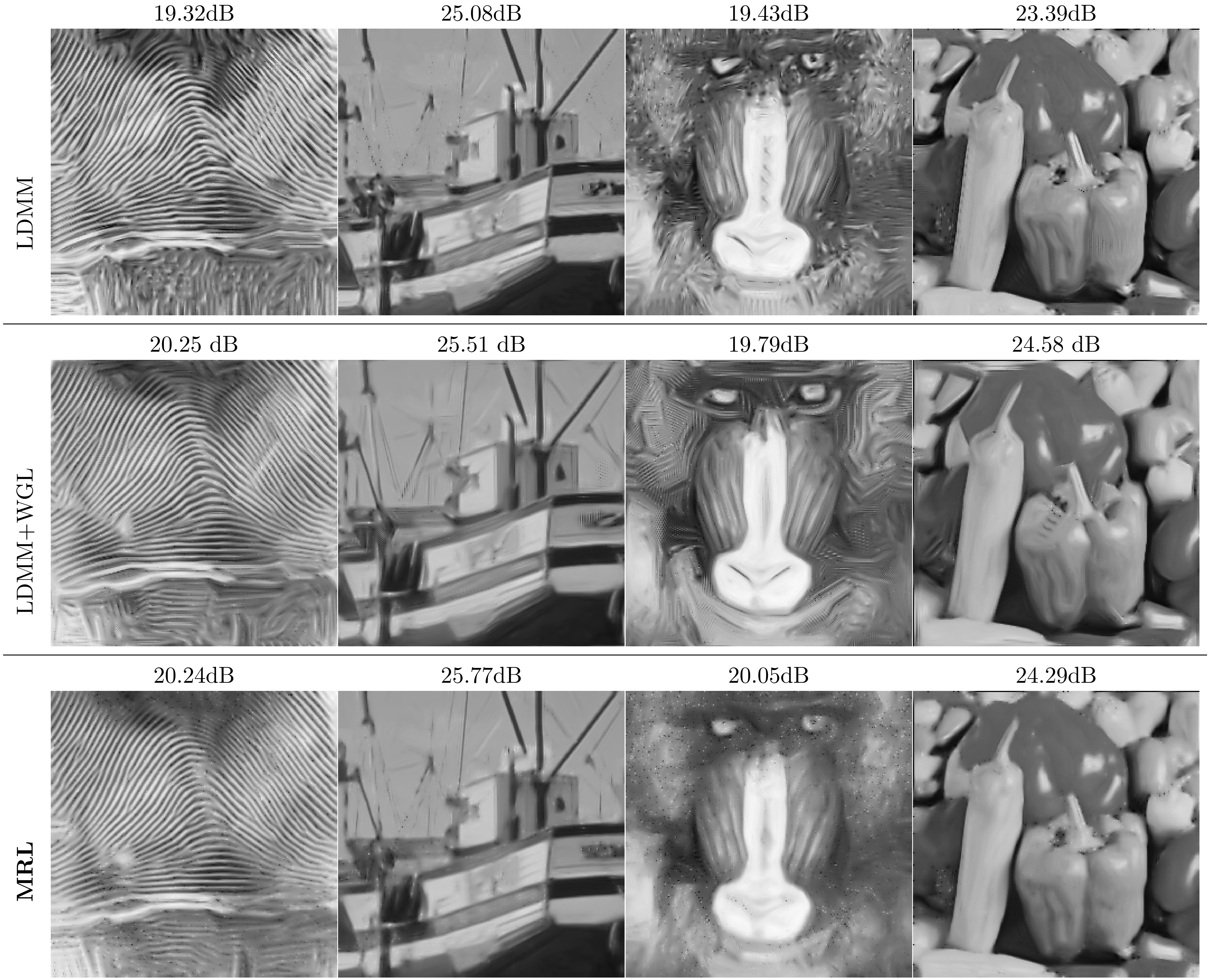

Image inpainting

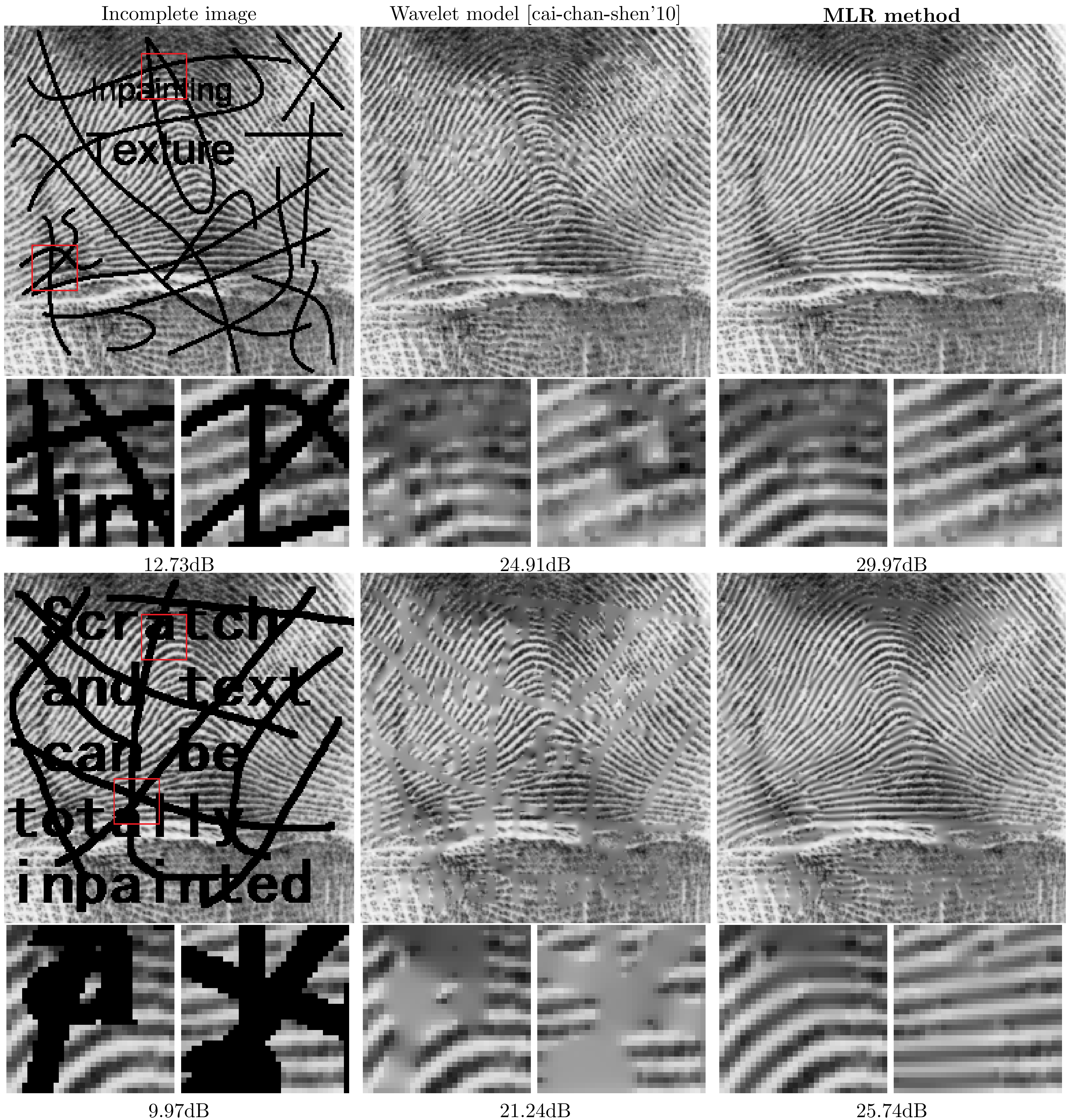

Super-resolution

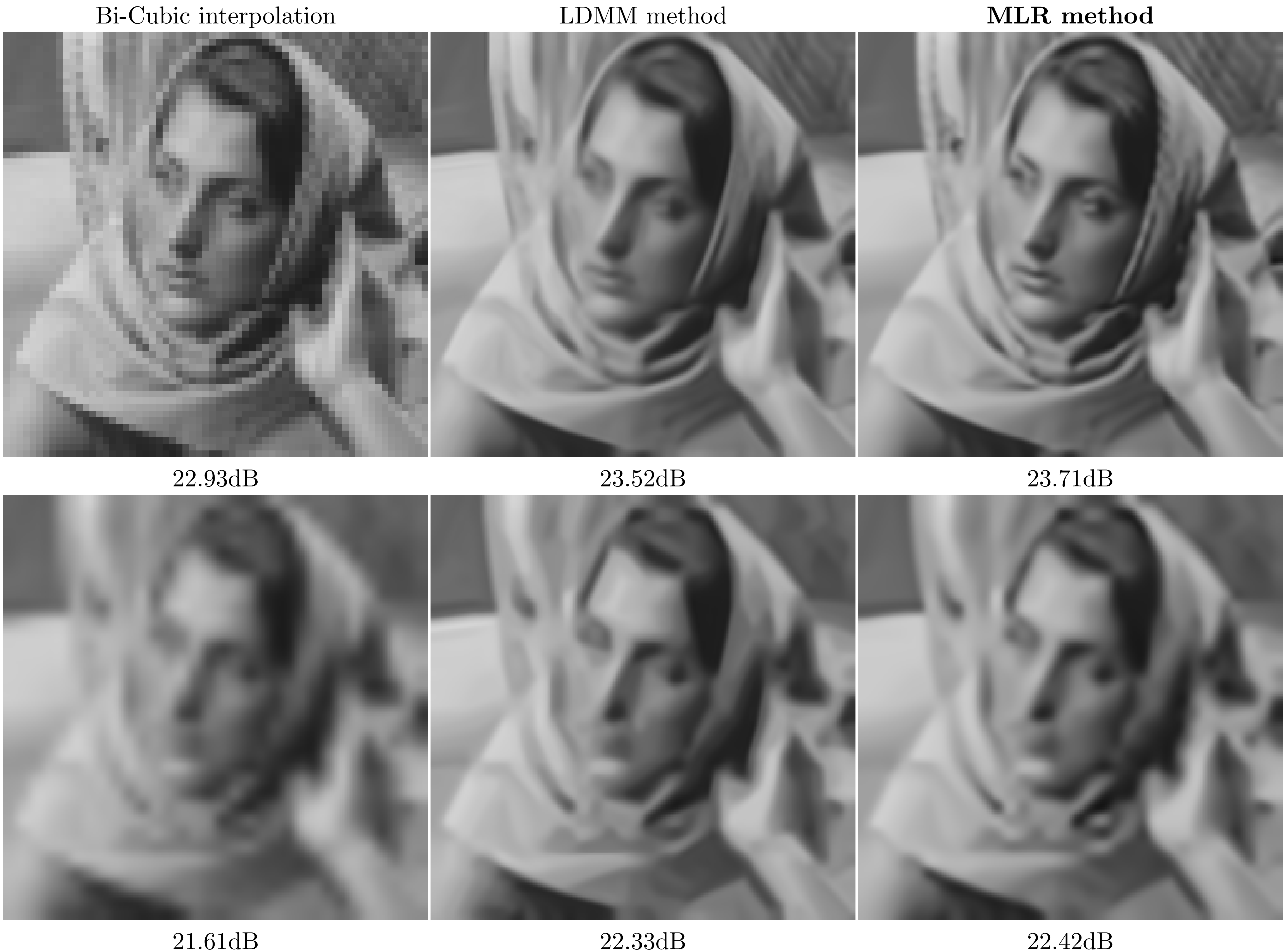

Figure 1: Super resolution from average. Down sample rate 4×4 and 8×8.

X-ray CT reconstruction

$$\min_{\mathcal{M}\subset\mathcal{R}^{\tau^2},f} \sum_{x\in\mathscr{I}} \|(R_{\mathcal{M},x})(\mathcal{P}(f))\|_*$$

$$\text{s.t.} \quad \mathcal{P}(f)\subset\mathcal{M}, \quad \mathcal{A}f = g.$$

where $g_i = \int_{\ell_i} \mu(\vec{r})\mathrm{d}\ell \approx \sum_{j=1}^{N_J} a_{ij} f_j = [\boldsymbol{A}f]_i$,

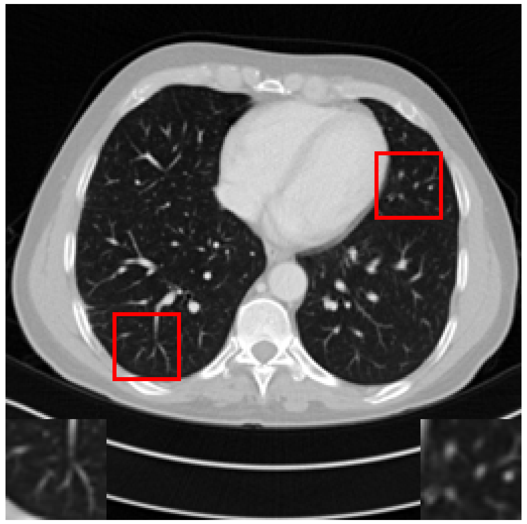

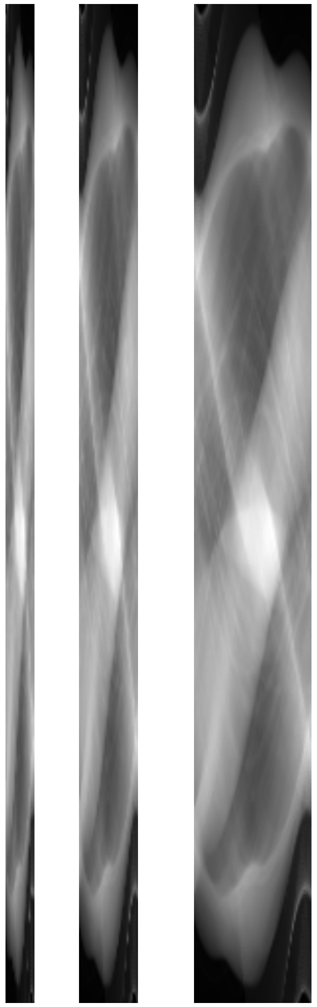

15 30 60

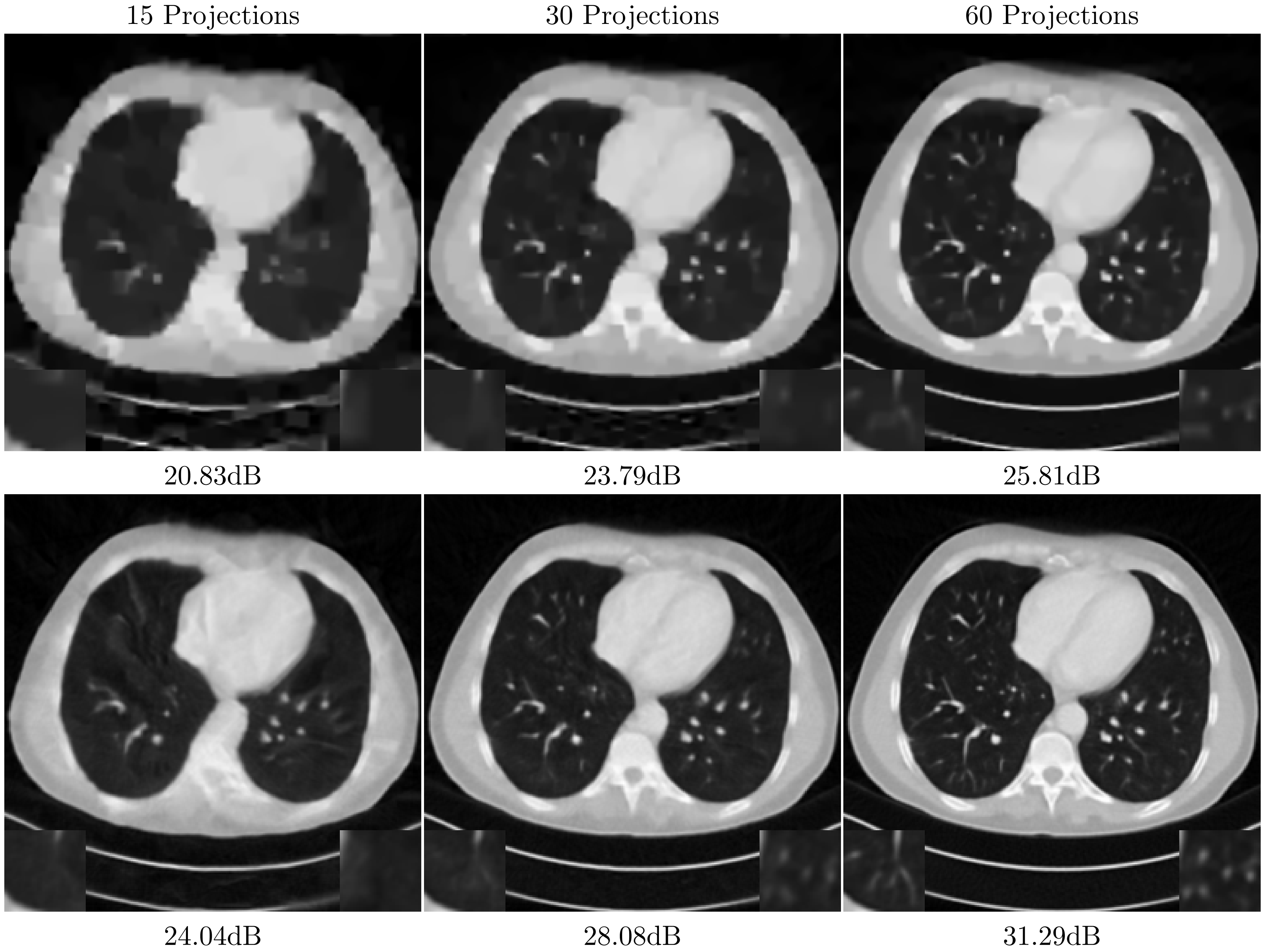

Figure 1: Fan-beam imaging for a clinical X-ray scanned chest slice from 15, 30 and 60 projection views. The second row: wavelet tight frame [DongLiShen2012]. The third row: the proposed MLR based method.

Summary

- We propose to use solutions of PDEs to understand geometric structure of data represented as incomplete inter-point distance.
- We develop a systematic way of computing PDEs on distance data sampled from manifolds.
- We also propose to use solutions of geometric PDEs to conduct global analysis, examples include global skeleton extraction, parameterization construction, and multi-scaled registration.
- We also consider extensions to image processing based on manifold low-rank regularization

Rongjie Lai, Jia Li and Abiy Tasissa, Exact Reconstruction of Distance Geometry Problem Using Low-rank Matrix Completion, preprint, 2017

Rongjie Lai and Jia Li, Manifold Based Low-rank Regularization for Image Restoration and Semi-supervised Learning, submitted, 2017

Rongjie Lai and Jia Li, Solving Partial Differential Equations on Manifolds From Incomplete Inter-Point Distanc. submitted, 2017.

Rongjie Lai, Jian Liang and Hongkai Zhao, A local mesh method for PDEs on point clouds, Inverse Problem and Imaging, 7(3), pp. 737-755, 2013.

Jian Liang, Rongjie Lai, Tsz Wai Wong and Hongkai Zhao, Geometric Understanding of Point Clouds Using Laplace-Beltrami Operator, CVPR 2012.

Thanks for your attention!

Rongjie Lai (lair@rpi.edu)

http://www.rpi.edu/~lair/

Rensselaer Polytechnic Institute